NASA TECHNICAL NOTE

NASA TN D-5829

c. 1

NASA TN D-5829

AN INVESTIGATION OF THE FINE-POINTING CONTROL SYSTEM OF A SOFT-GIMBALED ORBITING TELESCOPE

by Frederick R. Morrell

Langley Research Center
Hampton, Va. 23365

NATIONAL AERONAUTICS AND SPACE ADMINISTRATION • WASHINGTON, D. C. • JUNE 1970

1. Report No.	2. Government Accession No.	3. Recipient's Catalog No.
NASA TN D-5829		

4. Title and Subtitle

AN INVESTIGATION OF THE FINE-POINTING CONTROL SYSTEM OF A SOFT-GIMBALED ORBITING TELESCOPE

5. Report Date: June 1970

6. Performing Organization Code:

7. Author(s)

Frederick R. Morrell

8. Performing Organization Report No.: L-6988

9. Performing Organization Name and Address

NASA Langley Research Center
Hampton, Va. 23365

10. Work Unit No.: 125-19-10-05

11. Contract or Grant No.:

12. Sponsoring Agency Name and Address

National Aeronautics and Space Administration
Washington, D.C. 20546

13. Type of Report and Period Covered: Technical Note

14. Sponsoring Agency Code:

15. Supplementary Notes

The information presented herein was included in a thesis submitted in partial fulfillment of the requirements for the degree Master of Electrical Engineering, University of Virginia, Charlottesville, Virginia, March 1968.

16. Abstract

Computer-simulation results are presented for the rigid-body planar equations of motion of an attitude-stabilized orbiting telescope passively coupled to a manned service module. This coupling is provided through a set of soft springs and a two-axis gimbal alined with the telescope center of mass. Principal nonlinearities in the suspension system and the telescope control system are included. The simulation indicates feasibility of this operational mode.

17. Key Words (Suggested by Author(s))

Precision pointing for orbiting telescope
Control moment gyro
Attitude stabilization

18. Distribution Statement

Unclassified – Unlimited

19. Security Classif. (of this report)	20. Security Classif. (of this page)	21. No. of Pages	22. Price*
Unclassified	Unclassified	37	$3.00

*For sale by the Clearinghouse for Federal Scientific and Technical Information
Springfield, Virginia 22151

AN INVESTIGATION OF THE FINE-POINTING CONTROL SYSTEM OF A SOFT-GIMBALED ORBITING TELESCOPE*

By Frederick R. Morrell
Langley Research Center

SUMMARY

The fine-pointing control system of a telescope coupled to a manned service module through a gimbal and soft-spring suspension system is investigated, and the rigid-body equations of motion of the vehicle are presented for the planar case. The control system for the telescope consists of a single-axis, twin-rotor control moment gyroscope (CMG) as the momentum-exchange device and a high-gain pointing loop including a star sensor.

The rigid-body equations of motion of the vehicle for five degrees of freedom and the control systems for the telescope and the manned service module have been simulated on an analog computer. Also included in the simulation were crew-motion disturbance, environmental torques, nonlinearities in the CMG and suspension system, and noise in the telescope star sensor. The results of the simulation indicate that the telescope pointing requirement of approximately 0.01 second of arc can be achieved when a dither signal is applied to the CMG nonlinearity to reduce the effect of limit cycling in the telescope control system.

INTRODUCTION

One scientific field that can benefit from the proper use of space technology is astronomy. It has been estimated that a large orbiting telescope with a resolution equivalent to a diffraction-limited aperture of 120 inches (3 m) would provide significant improvement over the best ground-based facilities (refs. 1 and 2). Various sources have indicated that such a telescope should be designed around the basic Cassegrain configuration (refs. 1 and 2).

Figure 1 is an artist's concept of such a large telescope coupled to a manned service module. Because of the nature and complexity of the telescope, man's presence may be required for the assembly, initial alinement, and calibration of the telescope in space. There may be periods of time, therefore, during which the telescope will be required to operate while coupled to the manned service module.

*The information presented herein was included in a thesis submitted in partial fulfillment of the requirements for the degree Master of Electrical Engineering, University of Virginia, Charlottesville, Virginia, March 1968.

Since the angular resolution of a telescope with a diffraction-limited 120-inch-diameter (3-m) aperture is approximately 0.03 arc second, its pointing accuracy should be maintained at about 0.01 arc second to take full advantage of this resolution. The object of this investigation is to determine whether this pointing accuracy can be achieved when the telescope is coupled to the manned service module through a gimbal and soft-spring suspension system and subjected to the disturbances created by crew motion and the environment of a 300-nautical-mile (555.6-km) orbit. This study is an analog computer simulation of the rigid-body planar equations of motion of the vehicle, the telescope control system, the service-module control system, and nonlinearities in the suspension system and control system of the telescope.

SYMBOLS

D_g damping of telescope control moment gyro (CMG), lb-ft-sec/rad (N-m-sec/rad)

D_m damping of main gimbal, lb-ft-sec/rad (N-m-sec/rad)

d_1 distance from service module center of mass to spring attachment point (see fig. 2), ft (m)

d_2 radius of service module, ft (m)

d_3 radius of main gimbal, ft (m)

d_4 center-of-mass offset between main gimbal and telescope, in. (m)

F_X, F_Z force applied to translational degrees of freedom of vehicle (see fig. 2), lb (N)

H momentum of CMG, lb-ft-sec (N-m-sec)

I_g moment of inertia of telescope CMG gimbal, slug-ft^2 (kg-m^2)

I_X roll-axis moment of inertia of telescope, slug-ft^2 (kg-m^2)

I_Z yaw-axis moment of inertia of telescope, slug-ft^2 (kg-m^2)

I_1 pitch-axis moment of inertia of service module, slug-ft^2 (kg-m^2)

I_2	pitch-axis moment of inertia of telescope, slug-ft^2 (kg-m^2)
I_3	pitch-axis moment of inertia of main gimbal, slug-ft^2 (kg-m^2)
K	spring constant, lb/ft (N/m)
$K_{x,l}$	equivalent X-axis lower spring constant, lb/ft (N/m)
$K_{x,u}$	equivalent X-axis upper spring constant, lb/ft (N/m)
$K_{z,l}$	equivalent Z-axis lower spring constant, lb/ft (N/m)
$K_{z,u}$	equivalent Z-axis upper spring constant, lb/ft (N/m)
K_s	position-sensor gain, volts/arc second
K_t	compensation network and torque motor gain, lb-ft/volt (N-m/volt)
m_1	mass of space station, slugs (kg)
m_2	mass of telescope, slugs (kg)
m_3	mass of main gimbal, slugs (kg)
Q_i	generalized force, lb (N)
q_i	generalized coordinate
s	Laplacian operator, sec^{-1}
T_a	torque applied to CMG gimbal, lb-ft (N-m)
T_D	disturbance torques applied to telescope, lb-ft (N-m)
T_d	dither torque, lb-ft (N-m)
T_m	torque motor output, lb-ft (N-m)

T_1,T_2,T_3	torques applied to service module, telescope, and main gimbal, respectively, lb-ft (N-m)
t	time, sec
U	kinetic energy of vehicle
V	potential energy of vehicle
V_l	potential energy of lower spring sets
V_u	potential energy of upper spring set
x,z	translation of vehicle center of mass (fig. 2)
x_1,z_1	service-module translation (see fig. 2), ft (m)
x_2,z_2	telescope translation (see fig. 2), ft (m)
x_3,z_3	main-gimbal translation (see fig. 2), ft (m)
α	CMG gimbal angle, rad
Δ	incremental displacement, ft (m)
τ_s	star-sensor time constant, sec
ϕ_1	service-module pitch angle, rad
ϕ_2	telescope pitch angle, rad
ϕ_3	main-gimbal pitch angle, rad
ψ	spring mounting angle, rad
ω	orbital rate, rad/sec

Subscripts:

1 service module

2 telescope

3 main gimbal

Dots over symbols indicate derivatives with respect to time.

DESCRIPTION OF THE VEHICLE

A schematic of a soft-gimbaled orbiting telescope is shown in figure 2. The vehicle consists of three rigid bodies: a manned service module, a passive suspension system, and a 120-inch-diameter (3-m) telescope. The purpose of the suspension system is to isolate from the telescope any disturbances caused by man and his supporting facilities. The suspension-system concept analyzed here consists of an open truss connecting the service module to the telescope through a set of soft springs and a two-axis gimbal (see fig. 3). In the ideal case the centers of mass of the gimbal and the telescope coincide, since this decouples the rotational modes of the telescope from torques generated by the manned service module. Mass expulsion and equipment changes, however, would cause the center of mass of the telescope to shift as indicated by d_4 in figure 2. As a result of this shift, complete rotational decoupling of the telescope from the manned service module would not occur.

RIGID-BODY PLANAR EQUATIONS OF MOTION

The inertial reference frame x,z from which the rigid-body planar equations of motion are derived is located at the center of mass of the entire structure as shown in figure 2. The dynamics of the soft-gimbaled vehicle can be determined by considering the motion of each of the three rigid bodies. For the planar case, the vehicle nine degrees of freedom are reduced to seven by the bearing constraint between the telescope and the gimbal; this results in the following expression for kinetic energy of the vehicle:

$$U = \frac{1}{2} m_1\left(\dot{x}_1^2 + \dot{z}_1^2\right) + \frac{1}{2} m_2\left(\dot{x}_2^2 + \dot{z}_2^2\right) + \frac{1}{2} m_3\left(\dot{x}_2^2 + \dot{z}_2^2\right) - m_3 d_4 \dot{x}_2 \dot{\phi}_2 \sin \phi_2$$

$$+ m_3 d_4 \dot{z}_2 \dot{\phi}_2 \cos \phi_2 + \frac{1}{2} m_3 d_4^2 \dot{\phi}_2^2 + \frac{1}{2} I_1 \dot{\phi}_1^2 + \frac{1}{2} I_2 \dot{\phi}_2^2 + \frac{1}{2} I_3 \dot{\phi}_3^2 \qquad (1)$$

To find the expression for the potential energy of the vehicle, the equivalent spring constants must be determined for the planar case. A schematic representation for the spring suspension system is shown in figure 3. The spring sets are separated by 120^{o} and attach the crew-module truss structure to the gimbal. If the upper spring set is given a small displacement Δx, the resulting total force F_u generated by the spring set is

$$F_u = 2K \cos \psi \, \Delta x \tag{2}$$

The x-component of this spring force $F_{x,u}$ is

$$F_{x,u} = 2K \cos^2 \psi \, \Delta x \tag{3}$$

The z-component of force for the upper spring set in this case is zero. Similarly, if the gimbal is given a small displacement Δz,

$$F_{z,u} = 2K \sin^2 \psi \, \Delta z \tag{4}$$

The spring constants for the upper set of springs are taken from equations (3) and (4) as follows:

$$\left.\begin{aligned} K_{x,u} &= 2K \cos^2 \psi \\ K_{z,u} &= 2K \sin^2 \psi \end{aligned}\right\} \tag{5}$$

For the two lower sets of springs the inclination in the Z-axis must be taken into account. The equivalent spring constants for the two sets of lower springs are

$$\left.\begin{aligned} K_{x,l} &= 4K \cos^2 \psi \\ K_{z,l} &= 4K \sin^2 \psi \, \sin^2 \frac{\pi}{6} \end{aligned}\right\} \tag{6}$$

The potential energy of the vehicle caused by the spring sets can be found by referring to figure 2. For the upper spring set,

$$\begin{aligned} V_u = {} & K \cos^2 \psi \left(x_3 - d_3 \sin \phi_3 - x_1 - d_1 \cos \phi_1 + d_2 \sin \phi_1\right)^2 \\ & + K \sin^2 \psi \left[z_3 + d_3 \cos \phi_3 - z_1 - d_1 \sin \phi_1 - d_2 \cos \phi_1 \right. \\ & \left. - \left(d_3 - d_2\right)\right]^2 \end{aligned} \tag{7}$$

For the lower sets of springs,

$$V_l = 2K\cos^2\psi\left(x_3 + \frac{d_3}{2}\sin\phi_3 - x_1 - d_1\cos\phi_1 - \frac{d_2}{2}\sin\phi_1\right)^2$$
$$+ \frac{K}{2}\sin^2\psi\left[z_3 - \frac{d_3}{2}\cos\phi_3 - z_1 - d_1\sin\phi_1 + \frac{d_2}{2}\cos\phi_1\right.$$
$$\left.+ \left(\frac{d_3}{2} - \frac{d_2}{2}\right)\right]^2 \tag{8}$$

If the bearing constraint between the gimbal and the telescope is taken into account, the total potential energy V of the vehicle in the planar case is given by $V_u + V_l$:

$$V = K\cos^2\psi\left(x_2 - x_1 + d_4\cos\phi_2 - d_3\sin\phi_3 - d_1\cos\phi_1 + d_2\sin\phi_1\right)^2$$
$$+ 2K\cos^2\psi\left(x_2 - x_1 + d_4\cos\phi_2 + \frac{d_3}{2}\sin\phi_3 - d_1\cos\phi_1 - \frac{d_2}{2}\sin\phi_1\right)^2$$
$$+ K\sin^2\psi\left[z_2 - z_1 + d_4\sin\phi_2 + d_3\cos\phi_3 - d_1\sin\phi_1 - d_2\cos\phi_1\right.$$
$$\left.- (d_3 - d_2)\right]^2 + \frac{K}{2}\sin^2\psi\left[z_2 - z_1 + d_4\sin\phi_2 - \frac{d_3}{2}\cos\phi_3 - d_1\sin\phi_1\right.$$
$$\left.+ \frac{d_2}{2}\cos\phi_1 + \left(\frac{d_3}{2} - \frac{d_2}{2}\right)\right]^2 \tag{9}$$

The dissipation energy D of the system caused by viscous friction in the bearing connection between the telescope and the gimbal is

$$D = \frac{1}{2}D_m\left(\dot{\phi}_3 - \dot{\phi}_2\right)^2 \tag{10}$$

where D_m is the gimbal damping.

Equations (1), (9), and (10) represent the basic energy expressions of the vehicle for the planar case. When these expressions are substituted into Lagrange's equation (ref. 3)

$$\frac{d}{dt}\frac{\partial U}{\partial \dot{q}_i} - \frac{\partial U}{\partial q_i} + \frac{\partial V}{\partial q_i} + \frac{\partial D}{\partial \dot{q}_i} = Q_i \tag{11}$$

the expressions for the seven degrees of freedom become

$$\sum F_{x,1} = m_1\ddot{x}_1 - 6K\cos^2\psi\left(x_2 - x_1 + d_4\cos\phi_2 - d_1\cos\phi_1\right) \tag{12a}$$

$$\sum F_{x,2} = \left(m_2 + m_3\right)\ddot{x}_2 - m_3d_4\ddot{\phi}_2\sin\phi_2 - m_3d_4\dot{\phi}_2^2\cos\phi_2 + 6K\cos^2\psi\left(x_2 - x_1 + d_4\cos\phi_2 - d_1\cos\phi_1\right) \tag{12b}$$

$$\sum F_{z,1} = m_1\ddot{z}_1 - 3K\sin^2\psi\left[z_2 - z_1 + d_4\sin\phi_2 - d_1\sin\phi_1 + \frac{d_3}{2}\cos\phi_3 - \frac{d_2}{2}\cos\phi_1 - \frac{1}{2}\left(d_3 - d_2\right)\right] \tag{12c}$$

$$\sum F_{z,2} = \left(m_2 + m_3\right)\ddot{z}_2 + m_3d_4\ddot{\phi}_2\cos\phi_2 - m_3d_4\dot{\phi}_2^2\sin\phi_2 + 3K\sin^2\psi\left[z_2 - z_1 + d_4\sin\phi_2 - d_1\sin\phi_1 + \frac{d_3}{2}\cos\phi_3 - \frac{d_2}{2}\cos\phi_1 - \frac{1}{2}\left(d_3 - d_2\right)\right] \tag{12d}$$

$$\sum T_1 = I_1\ddot{\phi}_1 + 6Kd_1\cos^2\psi\sin\phi_1\left(x_2 - x_1 + d_4\cos\phi_2 - d_1\cos\phi_1\right) - 3Kd_2\cos^2\psi\cos\phi_1\left(d_3\sin\phi_3 - d_2\sin\phi_1\right) - 3Kd_1\sin^2\psi\cos\phi_1\left[z_2 - z_1 + d_4\sin\phi_2 + \frac{d_3}{2}\cos\phi_3 - \frac{d_2}{2}\cos\phi_1 - d_1\sin\phi_1 - \frac{1}{2}\left(d_3 - d_2\right)\right] + \frac{3}{2}Kd_2\sin^2\psi\sin\phi_1\left[z_2 - z_1 + d_4\sin\phi_2 + \frac{3}{2}d_3\cos\phi_3 - d_1\sin\phi_1 - \frac{3}{2}d_2\cos\phi_1 - \frac{3}{2}\left(d_3 - d_2\right)\right] \tag{12e}$$

$$\sum T_2 = \left(I_2 + m_3 d_4^2\right)\ddot{\phi}_2 - m_3 d_4 \ddot{x}_2 \sin \phi_2 + m_3 d_4 \ddot{z}_2 \cos \phi_2 - 6Kd_4 \cos^2\psi \sin \phi_2 \left(x_2 - x_1 + d_4 \cos \phi_2 - d_1 \cos \phi_1\right) + 3Kd_4 \sin^2\psi \cos \phi_2 \left[z_2 - z_1 + d_4 \sin \phi_2 - d_1 \sin \phi_1 + \frac{d_3}{2} \cos \phi_3 - \frac{d_2}{2} \cos \phi_1 - \frac{1}{2}\left(d_3 - d_2\right)\right] - D_m\left(\dot{\phi}_3 - \dot{\phi}_2\right) \tag{12f}$$

$$\sum T_3 = I_3 \ddot{\phi}_3 + 3Kd_3 \cos^2\psi \cos \phi_3 \left(d_3 \sin \phi_3 - d_2 \sin \phi_1\right) - \frac{3}{2} Kd_3 \sin \phi_3 \left[z_2 - z_1 + d_4 \sin \phi_2 - d_1 \sin \phi_1 + \frac{3}{2} d_3 \cos \phi_3 - \frac{3}{2} d_2 \cos \phi_1 - \frac{3}{2}\left(d_3 - d_2\right)\right] + D_m\left(\dot{\phi}_3 - \dot{\phi}_2\right) \tag{12g}$$

Although the equations of motion (12) are complicated and nonlinear, the vehicle would be stabilized to small angles; hence the first-order approximations $\sin \theta \to \theta$ and $\cos \theta \to 1$ are made and second-order products of rotational variables dropped. The simplified equations of motion are

$$\sum F_{x,1} = m_1 \ddot{x}_1 - 6K \cos^2\psi \left(x_2 - x_1 + d_4 - d_1\right) \tag{13a}$$

$$\sum F_{x,2} = \left(m_2 + m_3\right)\ddot{x}_2 + 6K \cos^2\psi \left(x_2 - x_1 + d_4 - d_1\right) \tag{13b}$$

$$\sum F_{z,1} = m_1 \ddot{z}_1 - 3K \sin^2\psi \left(z_2 - z_1 + d_4\phi_2 - d_1\phi_1\right) \tag{13c}$$

$$\sum F_{z,2} = \left(m_2 + m_3\right)\ddot{z}_2 + m_3 d_4 \ddot{\phi}_2 + 3K \sin^2\psi \left(z_2 - z_1 + d_4\phi_2 - d_1\phi_1\right) \tag{13d}$$

$$\sum T_1 = I_1 \ddot{\phi}_1 + 6Kd_1 \cos^2\psi \left(x_2 - x_1 + d_4 - d_1\right)\phi_1 - 3Kd_2 \cos^2\psi \left(d_3\phi_3 - d_2\phi_1\right) - 3Kd_1 \sin^2\psi \left(z_2 - z_1 + d_4\phi_2 - d_1\phi_1\right) + \frac{3}{2} Kd_2 \sin^2\psi \left(z_2 - z_1\right)\phi_1 \tag{13e}$$

$$\sum T_2 = \left(I_2 + m_3 d_4^2\right)\ddot{\phi}_2 - m_3 d_4 \ddot{x}_2 \phi_2 + m_3 d_4 \ddot{z}_2 - 6Kd_4 \cos^2\psi \left(x_2 - x_1 + d_4 - d_1\right)\phi_2 + 3Kd_4 \sin^2\psi \left(z_2 - z_1 + d_4\phi_2 - d_1\phi_1\right) - D_m\left(\dot{\phi}_3 - \dot{\phi}_2\right) \tag{13f}$$

$$\sum T_3 = I_3\ddot{\phi}_3 + 3Kd_3 \cos^2\psi\left(d_3\phi_3 - d_2\phi_1\right) - \frac{3}{2} Kd_3 \sin^2\psi\left(z_2 - z_1\right)\phi_3 + D_m\left(\dot{\phi}_3 - \dot{\phi}_2\right) \qquad (13g)$$

In the translational modes, it is apparent that the X-axis degrees of freedom are not influenced by the other modes; hence, the x_1 and x_2 degrees of freedom were dropped from further consideration. Since there is no form of natural damping in the translational modes, artificial means must be provided to limit oscillations. Damping must be provided for the pitch-axis rotation of the telescope ϕ_2 and the service module ϕ_1 by their respective control systems. For this analysis, a value of viscous damping torque D_m of 10 lb-ft-sec/rad (13.6 N-m-sec/rad), which might be achieved by passive means, was assumed to limit gimbal motion. This value of damping torque is a compromise between damping the gimbal highly and increasing the disturbance torques coupled to the telescope.

Table I indicates the major design values assumed for the parameters in this analysis (ref. 4).

External Disturbances

At an assumed orbit of 300 n. mi. (556 km), the predominant environmental disturbance acting on the vehicle is the gravity-gradient torque. This torque is a function of the yaw and roll moments of inertia of each body; it becomes a maximum value when the vehicle pitch axis is tilted 45° from the local vertical (ref. 5). The expression for the gravity-gradient torque is

$$T_g = \frac{3}{2} \omega^2\left(I_X - I_Z\right)\cos 2\omega t \qquad (14)$$

where ω is the orbital rate and I_X and I_Z are roll and yaw moments of inertia, respectively. The maximum magnitude of this environmental torque was calculated to be 0.25 lb-ft (0.34 N-m) acting on the telescope and 2.0 lb-ft (2.7 N-m) on the service module.

To simulate the maximum disturbance level created by crew motion, the torque on the manned service module was assumed to be 1200 lb-ft (1627 N-m) acting for 0.5 sec. This level would arise from a 193-lb (87.5 kg) man accelerating to 5 ft/sec (1.5 m/sec) in 0.5 sec at a 20-ft (6.1-m) moment arm. This motion was directed parallel to the Z-axis, since this generates the maximum disturbance to the telescope. The torque-time profile of the crew-motion disturbance is shown in figure 4.

Control System

To take advantage of the resolution capability of the telescope, ϕ_2 should be pointed to 0.01 arc second or better and maintained to this accuracy for long periods of time. A control system having large momentum storage and large torquing capability would thus be required to counteract both the long-period gravity-gradient disturbances and the short-period disturbances such as crew motion. The momentum-exchange device selected for this analysis was the twin-rotor, single-degree-of-freedom control-moment gyroscope (CMG) with passive gimbal dampers.

A simplified block diagram of the telescope-attitude control system, including a position sensor and compensation network in its attitude loop is shown in figure 5. The sensor in the attitude loop must operate from the main optics of the telescope and must be an inherently high-resolution device; typical requirements would be a gain K_S of 0.5 V per 0.01 arc second and a bandwidth of 5 Hz. To provide the necessary steady-state pointing accuracy for the telescope, the gain of the attitude loop, including the star-sensor gain, the compensation-network gain, and the torque-motor gain, was established as 10^5 lb-ft/rad (1.4×10^5 N-m/rad). The momentum H of each rotor of the CMG was chosen as 300 lb-ft-sec (407 N-m-sec). The ratio of CMG rotor momentum to gimbal inertia was assumed to be 2000, and the passive damping of the CMG gimbal was set at 0.5 lb-ft-sec/rad (0.7 N-m-sec/rad). Therefore, the damping ratio for the minor loop is 0.6 for CMG gimbal angles of 0^o and the resulting expression for the closed-loop attenuation, in arc second/lb-ft, is

$$\frac{\phi_2(s)}{T_D(s)} = \frac{1.7 \times 10^{-3}\left(\frac{s}{0.01}+1\right)\left(\frac{s}{3.31}+1\right)\left(\frac{s}{30}+1\right)^2\left(\frac{s}{31.4}+1\right)}{\left[\frac{s^2}{(1.07)^2}+\frac{s}{0.57}+1\right]\left[\frac{s^2}{(6.76)^2}+\frac{s}{7.42}+1\right]\left(\frac{s}{8.18}+1\right)\left[\frac{s^2}{(41.1)^2}+\frac{s}{21.6}+1\right]} \tag{15}$$

where the gyro gimbal angles have been set at 0^o and the telescope considered as a pure inertia. A plot of frequency response for the closed-loop case is shown in figure 6.

Since there are no stringent attitude-control requirements for the manned service module (e.g., 0.25^o maximum attitude error), its control system was greatly simplified. It consisted of a twin-rotor, single-axis CMG and a position-loop gain of 75 lb-ft/rad (102 N-m/rad). It was assumed for this study that the attitude and position of the service module relative to the telescope would be continuously updated to reduce disturbance to the telescope.

Allocation of Pointing Errors

An estimate of the telescope pointing errors which result from major sources can be obtained from the frequency response of the telescope control system shown in figure 6.

To obtain the telescope pointing errors listed in table II, the following assumptions were made: center-of-mass offset d_4 of 6 inches (0.15 m) between the main gimbal and the telescope, maximum main-gimbal velocity $\dot{\phi}_3$ of 7.5×10^{-3} rad/sec, translational offset $z_2 - z_1$ of 1.5 inches (0.04 m), service-module pointing error of 0.25^{o}, and maximum gravity-gradient disturbance torque on the telescope of 0.25 lb-ft (0.34 N-m). The predominant pointing error is caused by the main-gimbal damping since there is a relative lack of attenuation at that disturbance frequency (0.342 rad/sec). Table II indicates that in the linear case, the required pointing accuracy of 0.01 arc second for ϕ_2 can be met for the worst-case conditions considered here.

Nonlinearities

Because of the stringent accuracy specification on the telescope control system, the effect of nonlinearities on system stability and response becomes important. Two major nonlinearities have been considered: bearing friction in the CMG gimbals and bearing friction in the connection between the main-gimbal ring and the telescope.

References 4 and 5 have reported that for the size CMG being used here, the bearing static friction could be as low as 0.025 oz-in. (1.77×10^{-4} N-m) per gimbal. For the purpose of this analysis a static friction of 0.05 oz-in. (3.54×10^{-4} N-m) and a running friction of 0.025 oz-in. (1.77×10^{-4} N-m) per gimbal were assumed. The breakaway rate of the bearings was set at 4×10^{-5} rad/sec. Any viscous damping inherent in the gimbal bearings can be included in the passive gimbal damper D_g on the CMG. The CMG friction characteristics are shown in figure 7. At CMG gimbal rates below breakaway, the static friction prevents the gimbals from responding to torque motor inputs. During these periods the telescope is in effect uncontrolled and will drift until the attitude error is sufficiently large to provide the required torque to the gyro through the control-system high-gain attitude loop; therefore, a limit cycle will exist in the telescope control system.

Since the telescope control-system response should be linear for relatively low values of disturbance torque, adequate means must be provided to reduce the effect of the CMG static-friction dead band. There are several ways in which this reduction might be accomplished. First, an increase in the gain of the attitude loop in the vicinity of the limit-cycle frequencies would reduce the amplitude of the telescope-attitude limit cycle and would extend the bandwidth of the control system. This method would provide marginal performance, at best, for reasonable values of gain in the feedback loop. A second method, which would effectively eliminate the static-friction dead band, would be to apply a dither signal to the CMG gimbal axis. This technique is reported in the literature

(ref. 6). The frequency and amplitude of the dither torque T_d must be determined from the frequency response of the telescope control system shown in figure 6 and consideration of dither torque necessary to maintain zero crossing of the CMG gimbal velocity.

For the purpose of this investigation, the static friction in the bearing connection between the main-gimbal ring and the telescope was assumed to be 0.192 oz-in. (1.36×10^{-3} N-m), and the Coulomb friction was set at one-half this value.

The effect of the static-friction dead band causes jerks in the relative velocity between the main gimbal and the telescope. When operating within the static-friction dead band, the telescope and the main gimbal move together. The motions of the telescope will be confined to 0.01 arc second; beyond this range the telescope control system would develop the torque necessary to break the static-friction dead band.

RESULTS OF ANALOG COMPUTER SIMULATION

Linear System

The equations of motion and the control systems were simulated on an analog computer. To provide a basis on which to judge the response of the vehicle, the simulation results for the linear system are considered first. Figure 8 shows the real-time response of significant variables for the telescope-linear control system to a step input of 0.25 lb-ft (0.34 N-m) with the control moment gyro (CMG) gimbal set at 0^o. The steady-state attitude ϕ_2 of the telescope for this condition is 0.0004 arc second. The effective applied torque T_a to the gyro in the steady state is approximately 0.04 oz-in. (2.8×10^{-4} N-m), and the steady-state velocity of the CMG gimbal $\dot{\alpha}$ is 4.16×10^{-4} rad/sec (0.024 deg/sec).

Figure 9 illustrates the response of the entire vehicle to the crew-motion disturbance of 1200 lb-ft (1627 N-m) torque (fig. 4) and 60 lb (267 N) force. The displacement d_4 between the telescope and gimbal centers of mass in this case and all cases to follow is 6 inches (0.15 m). The telescope CMG gimbal was set at 0^o, and no environmental torques were considered. After the initial overshoot of 0.0012 arc second of the telescope as a result of the crew-motion disturbance, the telescope control system followed the coupling torques of the main gimbal and translational degrees of freedom. The overshoot of the service-module attitude angle ϕ_1 to the crew-motion disturbance was 6×10^{-4} rad (0.035^o). The main-gimbal velocity $\dot{\phi}_3$ achieved a maximum of 1.5×10^{-4} rad/sec, and its motion was completely damped in approximately 240 seconds. The translational difference $z_2 - z_1$ was a maximum of 0.244 inch (6.2×10^{-3} m) and was lightly damped. This translational-mode damping resulted from a fortuitous choice

of parameters in the vehicle design; this damping can be predicted from a root locus of the characteristic equation of the vehicle (ref. 5). Other means of providing effective damping for the vehicle should be investigated.

For the run shown in figure 10, the conditions were the same as those in figure 9 except that an initial condition of 1.74×10^{-2} rad (1.0^{o}) was imposed on the main-gimbal attitude ϕ_3. The crew-motion torque was delayed to show more clearly its effect on the telescope response. The peak overshoot of the telescope attitude ϕ_2 to the crew-motion disturbance in the service module was 0.0023 arc second, and the peak torque input to the telescope caused by the main gimbal was 3.0×10^{-2} lb-ft (4.07×10^{-2} N-m). For the final run made under linear conditions, shown in figure 11, the initial conditions were a service-module attitude ϕ_1 of 4.3×10^{-3} rad (0.25^{o}) and a main-gimbal attitude ϕ_3 of 1.74×10^{-2} rad (1.0^{o}). The crew-motion disturbance was applied when the service-module attitude reached 1.74×10^{-3} rad (0.1^{o}). The peak overshoot of the telescope attitude for this run was 0.0022 arc second.

Since the response of the telescope to the imposed conditions was within specifications, the feasibility of the soft-gimbaled mode of operation under idealized conditions has been established. It should be noted, however, that only one crew-motion disturbance was considered in this analysis. It is evident from figures 9 to 11 that unrestricted frequency of crew motion may increase the amplitude of oscillation of the lightly damped translational mode to unacceptable values. For this reason, some additional form of damping should be provided for this degree of freedom.

Nonlinear System

To provide a more realistic appraisal of vehicle performance, the nonlinearities of the telescope control moment gyro bearings and the main gimbal bearings were also included in the analog simulation. For the CMG bearings, the static friction was simulated at 0.05 oz-in. (3.5×10^{-4} N-m), and the Coulomb friction, at 0.025 oz-in. (1.77×10^{-4} N-m). For the main-gimbal bearings, the static-friction level was simulated at 0.192 oz-in. (1.36×10^{-3} N-m), and the Coulomb friction level, at 0.096 oz-in. (6.8×10^{-4} N-m).

Figure 12 illustrates the limit cycles which occur in the telescope control system when no external torques are applied. The drift in attitude ϕ_2 is caused by a small telescope rate. When this rate causes the attitude error to increase to a sufficiently large value to cause the torque motor to break the static-friction dead band, a control torque will be applied to the telescope. Because there is insufficient attitude error to maintain the gyro free of the static-friction dead band, a limit cycle results. For the gyro gimbals set at 0^{o} with no applied torques, as in figure 12, the limit-cycle frequency is 1.29 rad/sec at an amplitude of ±0.026 arc second. Figure 13 shows that when an

external torque is applied to the telescope, the frequency of the limit cycle increases while the amplitude of the telescope attitude decreases. The highest frequency attained (fig. 13) is 5.45 rad/sec and the amplitude is 0.0035 to -0.002 arc second for a step input of 0.0455 lb-ft (6.2×10^{-2} N-m) and with the gyro gimbals set at 0^{o}.

The effect of the main-gimbal nonlinearity is shown in figure 14. The disturbance on the vehicle was caused by crew-motion and environmental torques of 0.01 lb-ft (1.36×10^{-2} N-m) on the telescope and 0.1 lb-ft (1.36×10^{-1} N-m) on the service module. The gimbal remained at a constant offset of 5×10^{-5} rad (0.0029^{o}) when gimbal motion ceased; this provided a constant torque input to the service module of 1.5×10^{-3} lb-ft (2.03×10^{-3} N-m). It is apparent that no deleterious effects are encountered for the nonlinearity of the main-gimbal bearings at the friction levels specified.

Figure 14 also indicates the limit cycle in the telescope resulting from the CMG static-friction dead band and the low torque levels. The CMG gimbal was set at 45^{o}; therefore, the effective attitude-loop gain was reduced by 0.707 for this run. The amplitude of the telescope-attitude limit cycle reached a peak value of 0.034 arc second. To correct this situation, a dither signal with a torque amplitude of 0.75 oz-in. (5.30×10^{-3} N-m) and a frequency of 38 rad/sec was applied to the CMG and the result is illustrated by figure 15. The conditions for this case are identical with those in figure 14. After the initial overshoot caused by the step function and dither signal, the telescope responded to the crew-motion disturbance with an overshoot of 0.0025 arc second.

The vehicle response indicated by figure 16 was for the following conditions: (1) environmental torques of 2.0 lb-ft (2.71 N-m) on the service module and 0.25 lb-ft (0.34 N-m) on the telescope; (2) initial conditions of 4.3×10^{-3} rad (0.25^{o}) on the service module and 1.74×10^{-2} rad (1.0^{o}) on the main gimbal; and (3) telescope CMG gimbal set at 45^{o}. The crew-motion disturbance was applied when the service-module attitude was 2.3×10^{-3} rad (0.13^{o}). After the first overshoot of the telescope response to the initial conditions and the environmental torques, the telescope-attitude error did not exceed 0.005 arc second. The corresponding case with the addition of a dither signal of 0.75 oz-in. (5.3×10^{-3} N-m) at 38 rad/sec is shown in figure 17. In this case the maximum overshoot of the telescope after the initial response was 0.008 arc second. The additional error of 0.003 arc second in the telescope attitude occurred because the CMG gimbal velocity $\dot{\alpha}$ was close to the breakout velocity of 4×10^{-5} rad/sec for a short period of time. This increased overshoot, however, was within the pointing specification of the telescope of 0.01 arc second.

The final three figures are used to illustrate the effects of noise in the output of the star-position sensor of the telescope. For the cases considered here, the noise amplitude was equivalent to 0.003 arc second rms and was inserted at the input of the filter

representing the star-sensor transfer function. The noise source was provided by a low-frequency Gaussian noise generator which produced a flat relative spectral density from 0 to 35 Hz. Figure 18 indicates the response of the vehicle with noise added to the conditions of figure 14. The dithering effect of the noise maintained the attitude ϕ_2 of the telescope within 0.01 arc second; however, the performance was marginal. The addition of a dither signal of 0.75 oz-in. (5.3×10^{-3} N-m) at 38 rad/sec in the presence of this noise dramatically improved the telescope pointing accuracy, as illustrated by figure 19.

The final case considered illustrates the addition of 0.003 arc second rms noise and a dither signal of 0.75 oz-in. (5.3×10^{-3} N-m) at 38 rad/sec to the case shown in figure 16. These conditions represent the most severe case encountered for this analysis. The resulting system response is shown in figure 20 and indicates that the pointing specifications can be met when the telescope, with its major nonlinearities included, is subjected to a severe disturbance environment.

CONCLUDING REMARKS

Analysis and computer simulation have demonstrated that the attitude control of a space telescope coupled to a service module through a suspension system appears feasible. The simulation of the rigid-body planar equations of motion of the vehicle indicates that the pointing accuracy of the telescope can be maintained within the prescribed 0.01 arc second when the vehicle is subjected to severe disturbance torques.

Since the closed-loop attenuation of the telescope control system is minimal at the main-gimbal frequency of 0.342 rad/sec, it is advisable to redesign the attitude-loop compensation network or to increase the attitude-loop gain to reduce the effect of disturbance at that frequency.

The results indicate that some form of damping should be provided for the translational modes of the vehicle, because unrestricted crew motion could increase the lightly damped oscillations to intolerable levels.

The disturbances applied to the telescope represent the worst-case conditions expected. The center-of-mass offset between the main-gimbal ring and the telescope in all cases was 6 inches (0.15 m). In practice this distance may be reduced to less than 1 inch (0.025 m) by means of manual or automatic control. The crew-motion disturbance of 1200 lb-ft (1627 N-m) torque and 60 lb (267 N) force which is coupled to the telescope through the suspension system is considered by previous studies to be the most severe level expected.

The static-friction dead band caused by the bearings of the control moment gyro creates a limit cycle in the telescope control system when low torque levels are experienced. This situation can be corrected by employing a dither signal whose amplitude is

sufficient to prevent the control moment gyro gimbal from dwelling near zero velocity and whose frequency is sufficiently attenuated by the closed-loop response of the control system to limit the resulting periodic variation in the telescope pointing angle to small levels.

The main-gimbal damping may be varied depending on the response of the telescope control system to the frequency of its disturbance. A more meaningful appraisal of this damping could be accomplished if more adequate information concerning crew-motion frequency were available.

Langley Research Center,
National Aeronautics and Space Administration,
Hampton, Va., April 6, 1970.

REFERENCES

1. Spitzer, Lyman, Jr.: Astronomical Research With the Large Space Telescope. Science, vol. 161, no. 3838, July 19, 1968, pp. 225-229.

2. Joint Space Panels: The Space Program in the Post-Apollo Period. U.S. Govt. Printing Office, Feb. 1967.

3. McCuskey, S. W.: Introduction to Advanced Dynamics. Addison-Wesley Pub. Co., Inc., c.1959.

4. Anon.: A System Study of a Manned Orbital Telescope. D2-84042-1 (Contract NAS1-3968), Boeing Co., Oct. 1965.

5. Anon.: A System Study of a Manned Orbital Telescope – Synchronous Orbit Study. D2-84042-2 (Contract NAS1-3968), Boeing Co., Apr. 1966.

6. Cosgriff, Robert Lien: Nonlinear Control Systems. McGraw-Hill Book Co., Inc., 1958.

TABLE I.- ASSUMED PARAMETERS FOR TELESCOPE COUPLED TO A MANNED SERVICE MODULE

Manned-service-module mass, m_1	3835.1 slugs (55 969 kg)
Telescope mass, m_2	673.9 slugs (9835 kg)
Gimbal mass, m_3	8.695 slugs (126.9 kg)
Service-module pitch-axis inertia, I_1	6.09×10^5 slug-ft^2 (8.26×10^5 kg-m^2)
Telescope pitch-axis inertia, I_2	1.58×10^5 slug-ft^2 (2.14×10^5 kg-m^2)
Gimbal pitch-axis inertia, I_3	221.7 slug-ft^2 (300 kg-m^2)
Distance from c.m. of service module to spring attachment, d_1	42.8 ft (13.1 m)
Radius of service module, d_2	8.15 ft (2.48 m)
Radius of gimbal, d_3	7.13 ft (2.17 m)
Spring constant, K	0.5088 lb/ft (7.425 N/m)
Spring mounting angle, ψ	0.955 radian

TABLE II.- ALLOCATION OF TELESCOPE POINTING ERRORS FOR DETERMINISTIC DISTURBANCES

Source	Torque		Pointing error contribution, arc second
	lb-ft	N-m	
Main-gimbal damping	0.075	0.102	0.005
Translational coupling	.064	.087	.0004
Service-module pointing error	.095	.128	.0002
Gravity gradient	.25	.339	.0004

Figure 1.- Artist's conception of soft-gimbaled vehicle. L-70-1570

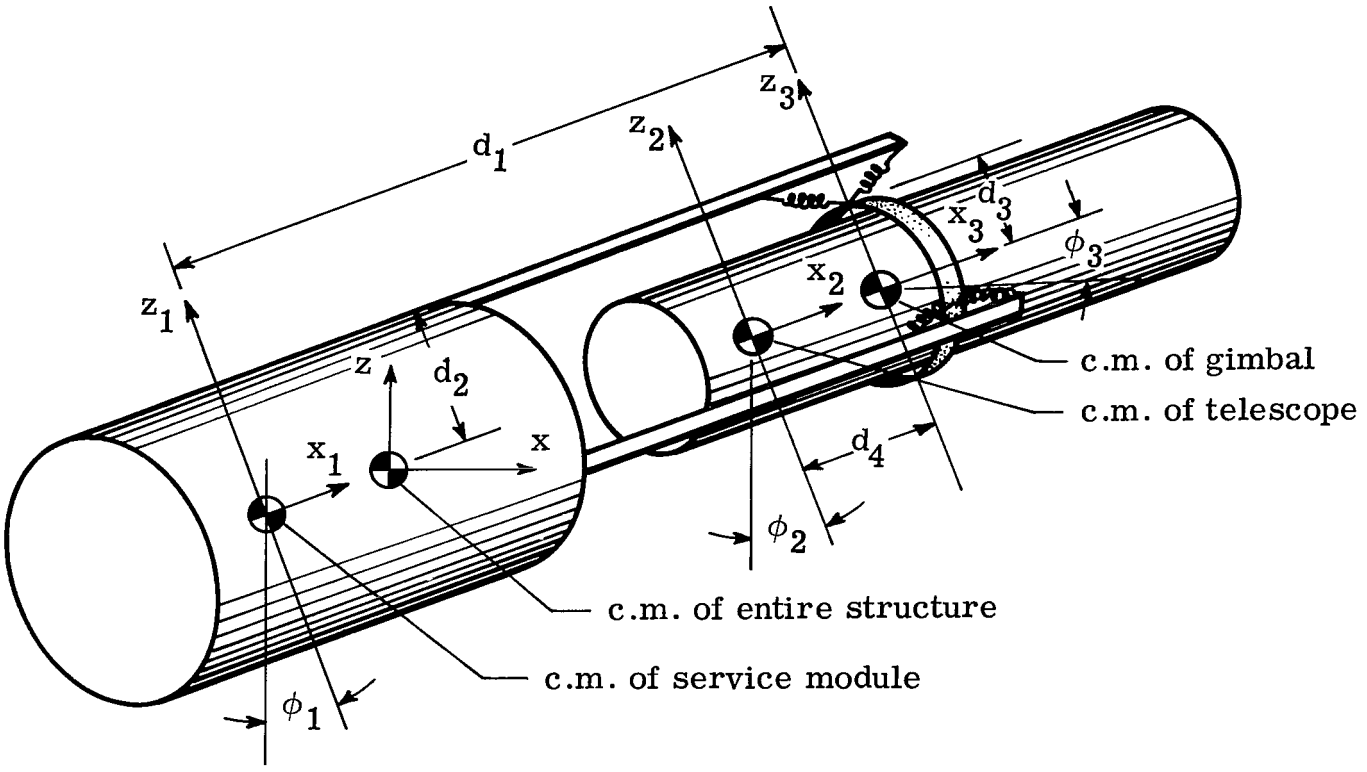

Figure 2.- Schematic of soft-gimbaled telescope.

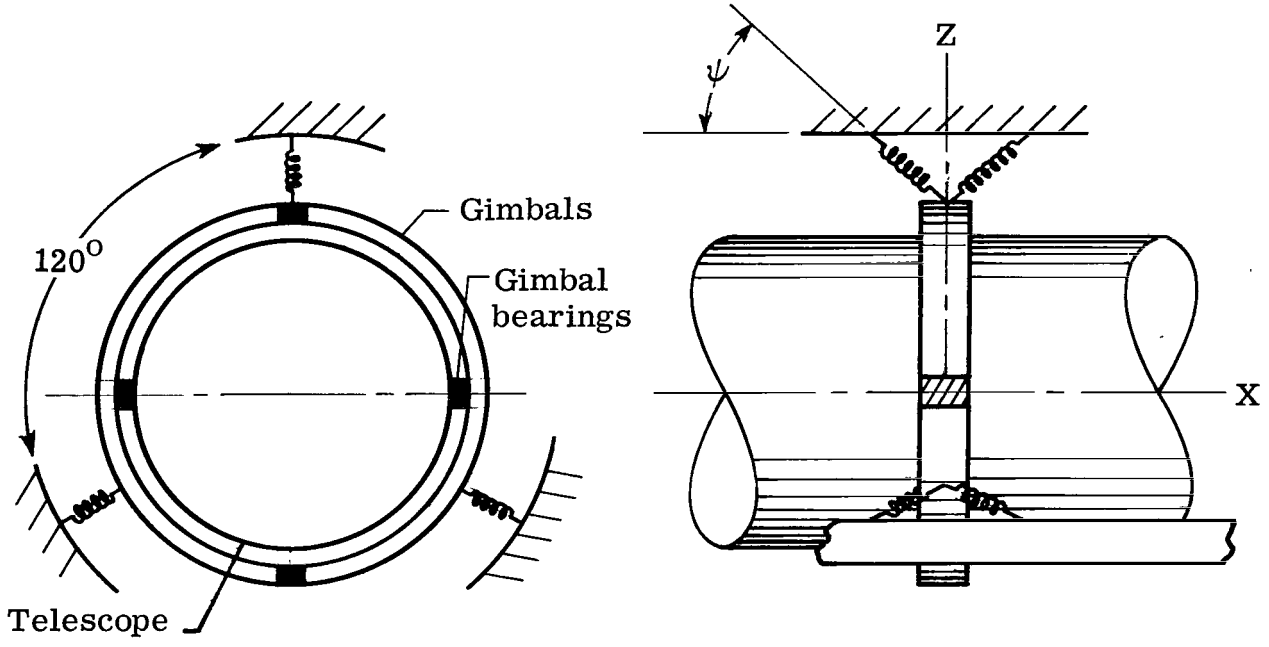

Figure 3.- Schematic of soft-gimbaled suspension system.

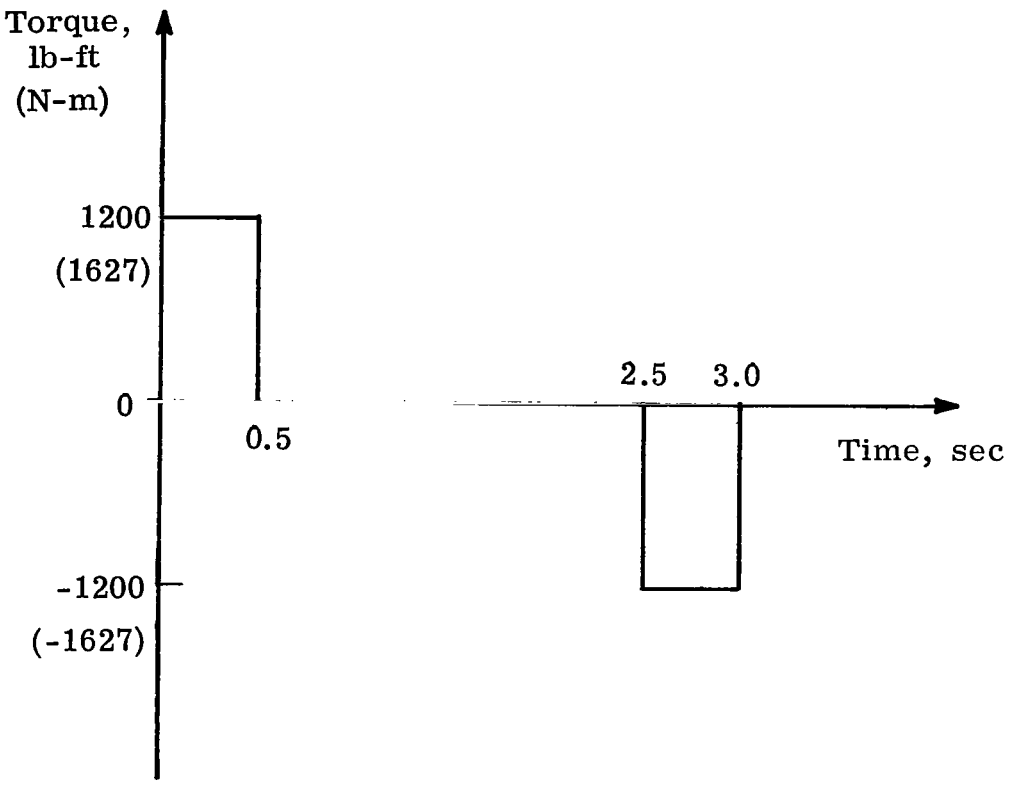

Figure 4.- Torque-time profile of crew motion.

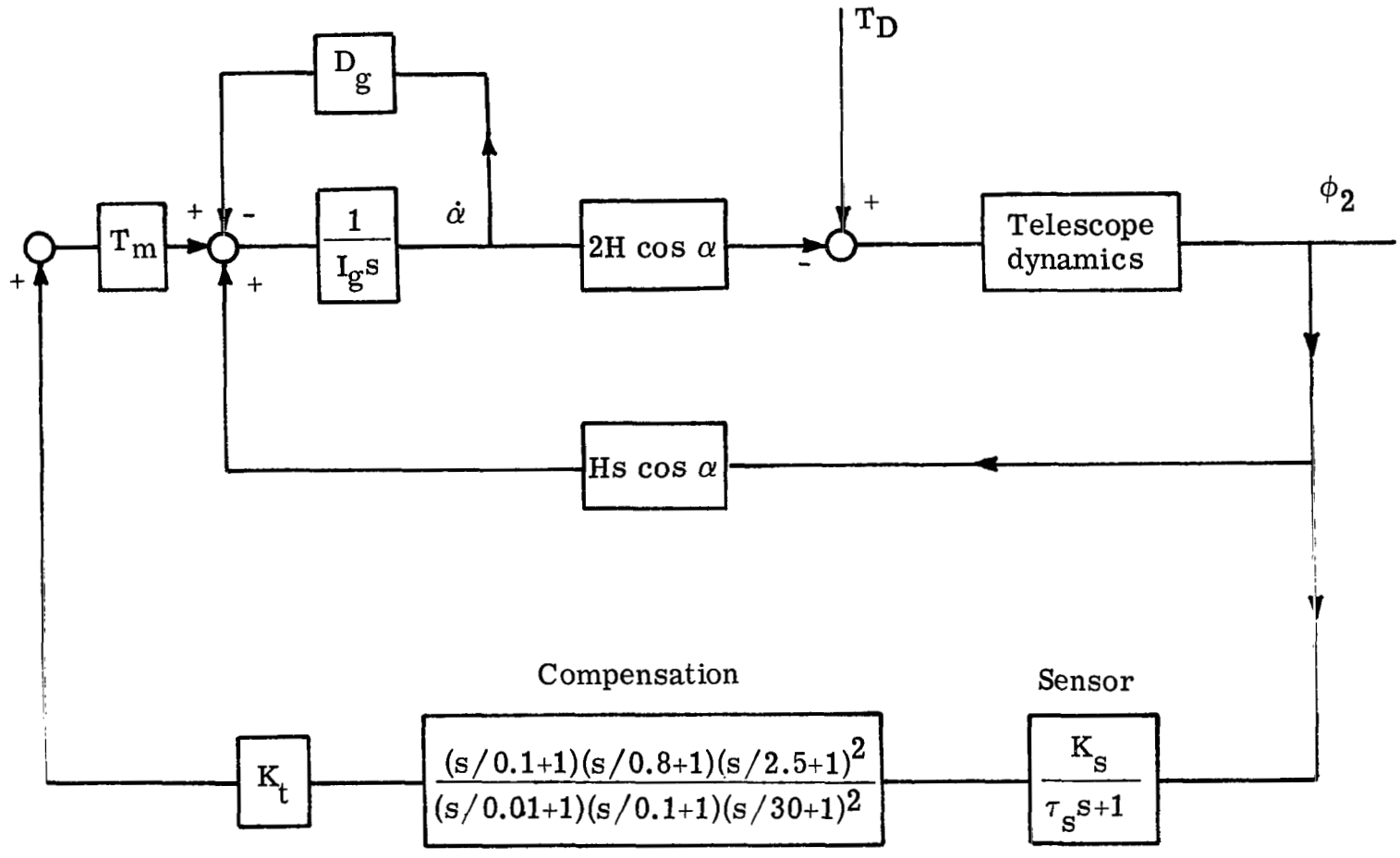

Figure 5.- Block diagram of telescope-attitude control system.

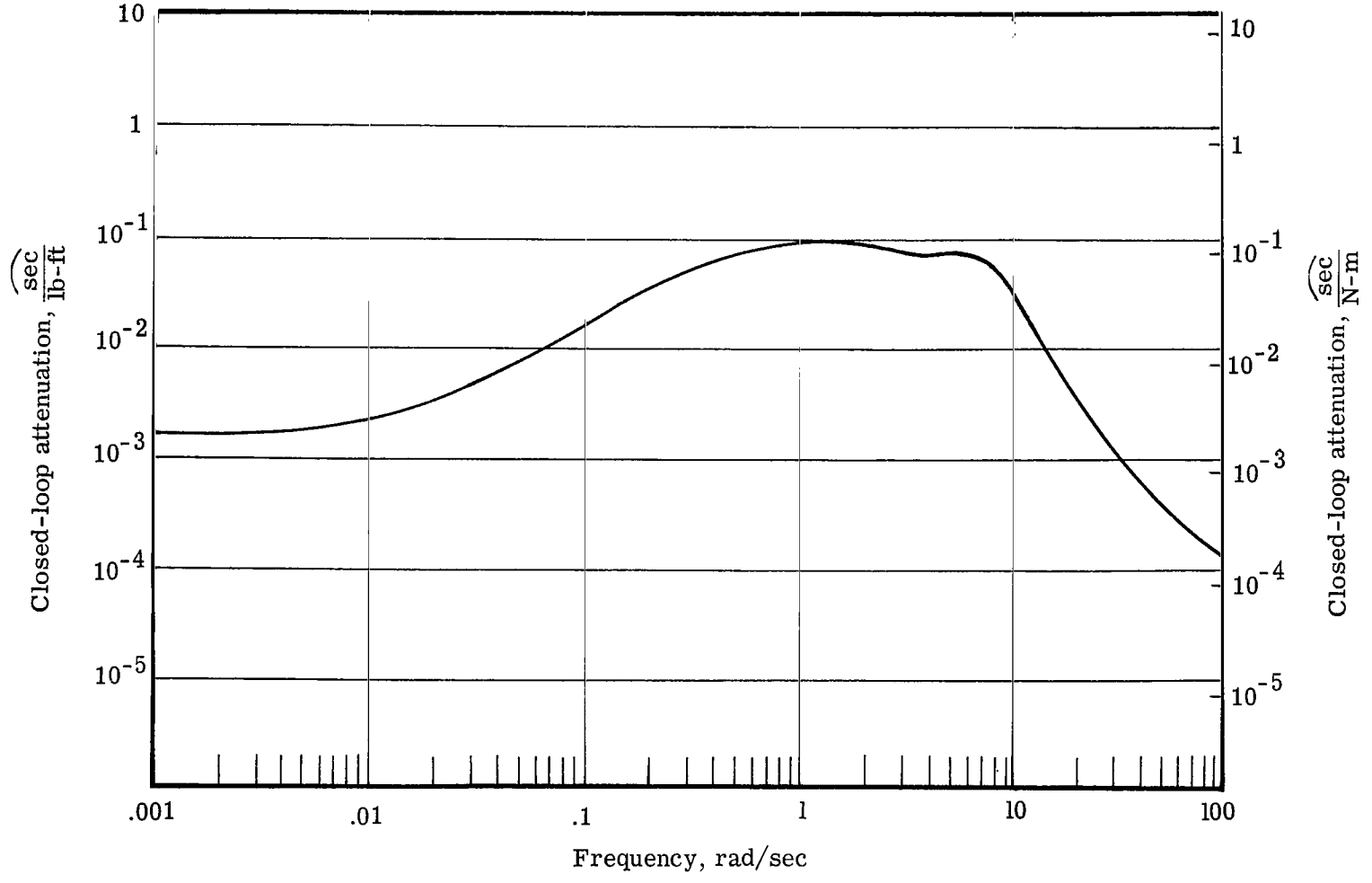

Figure 6.- Closed-loop attenuation for telescope control system.

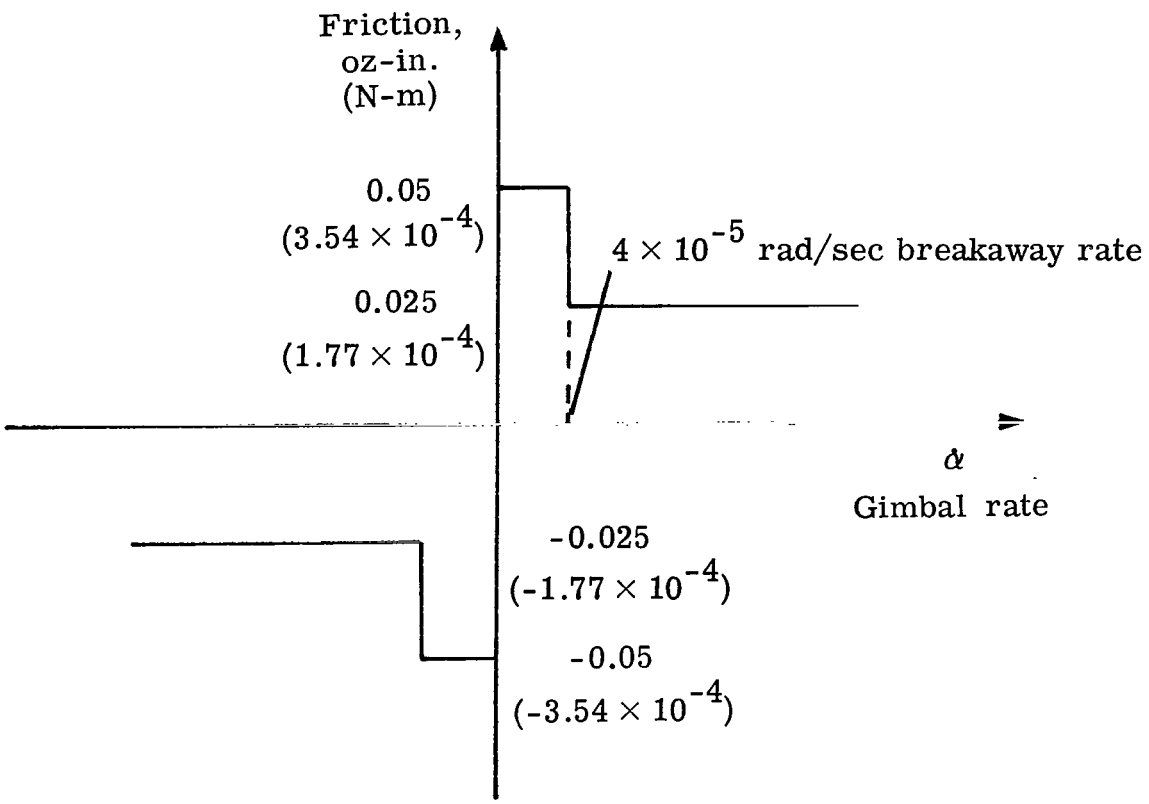

Figure 7.- CMG bearing-friction characteristic.

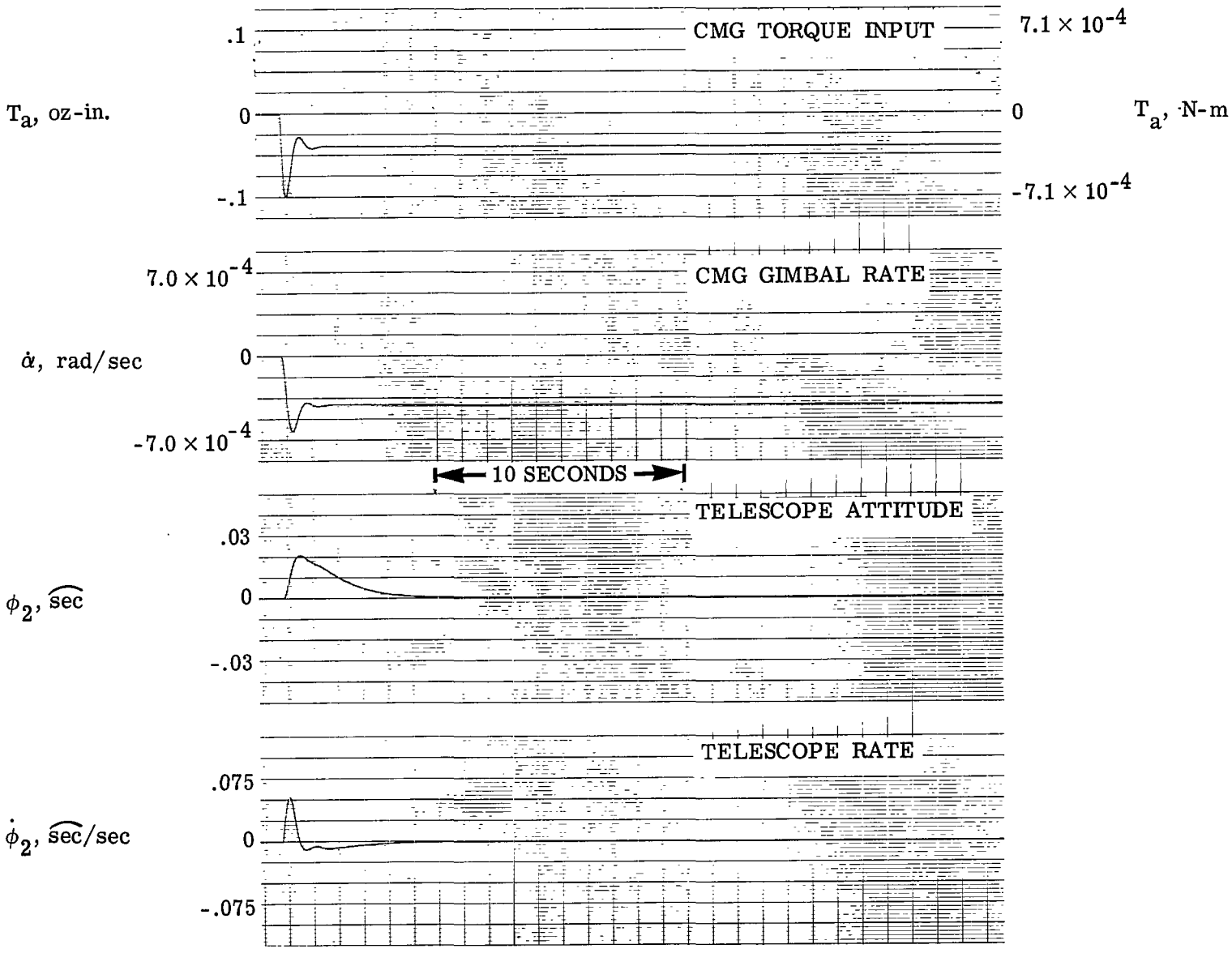

Figure 8.- Response of telescope control system to step input of 0.25 lb-ft (0.34 N-m). CMG gimbal set at 0^0.

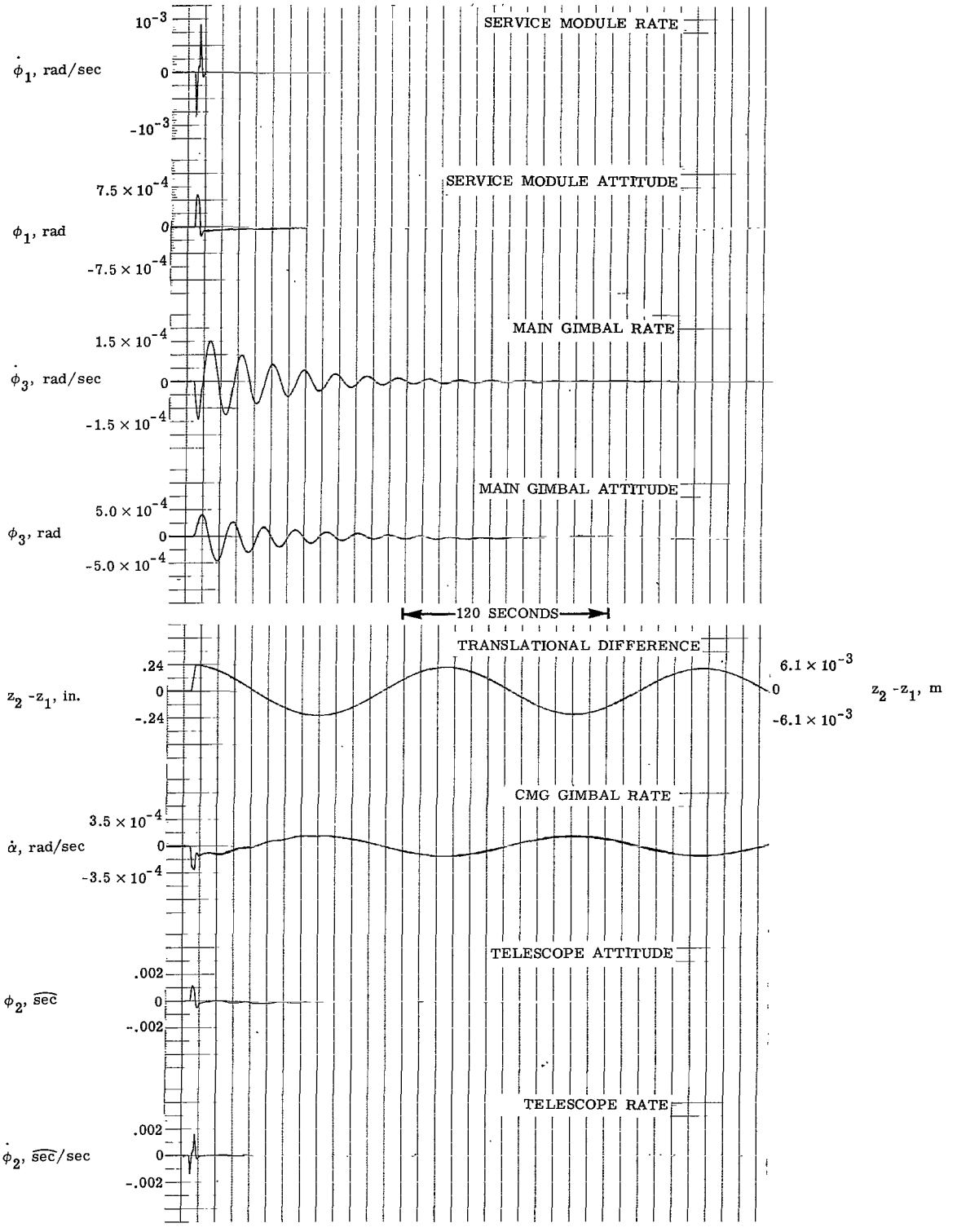

Figure 9.- Response of vehicle to crew-motion disturbance. CMG gimbal set at 0°.

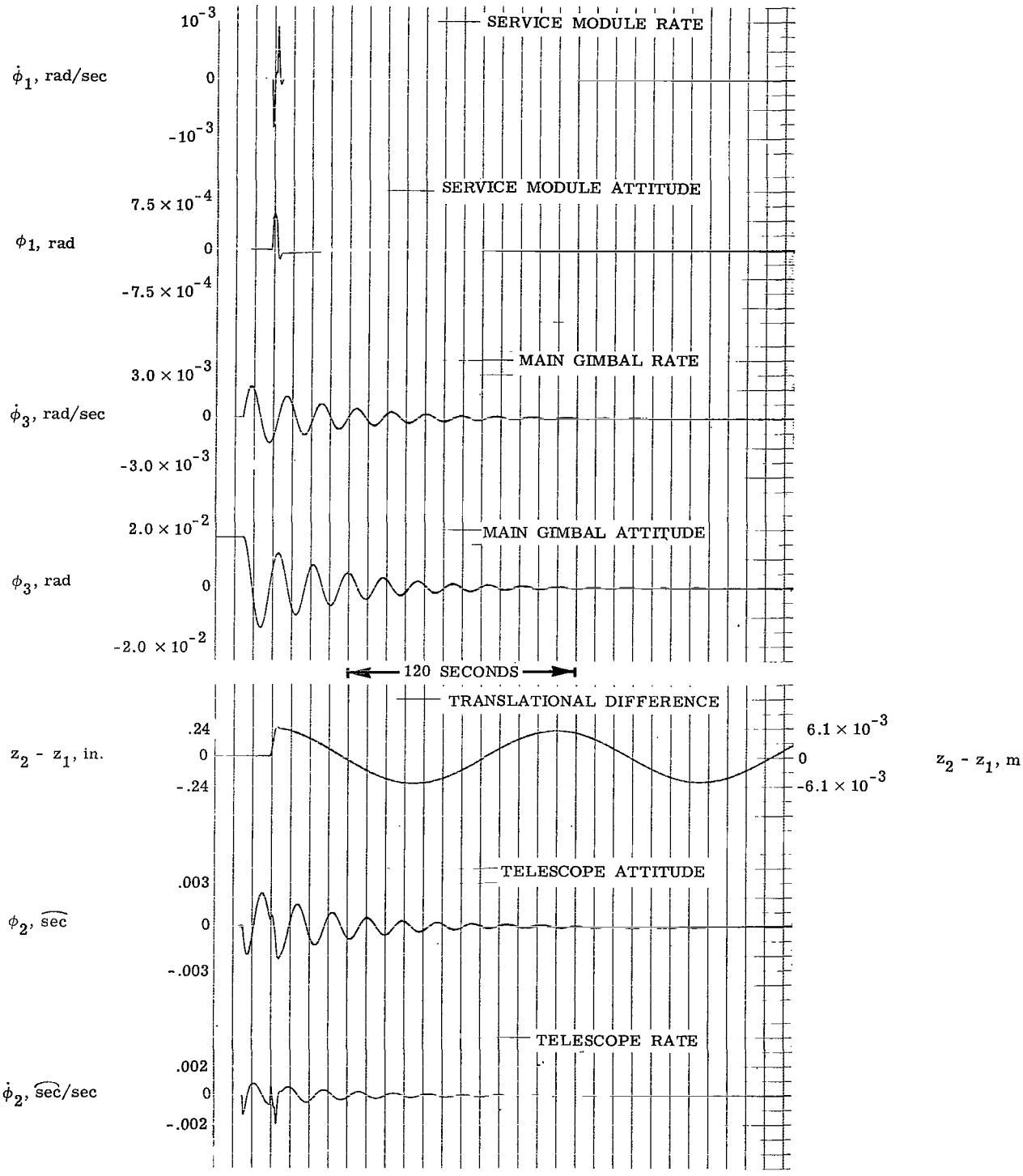

Figure 10.- Response of vehicle to crew-motion disturbance and initial condition of 1^0 on main-gimbal attitude. CMG gimbal set at 0^0.

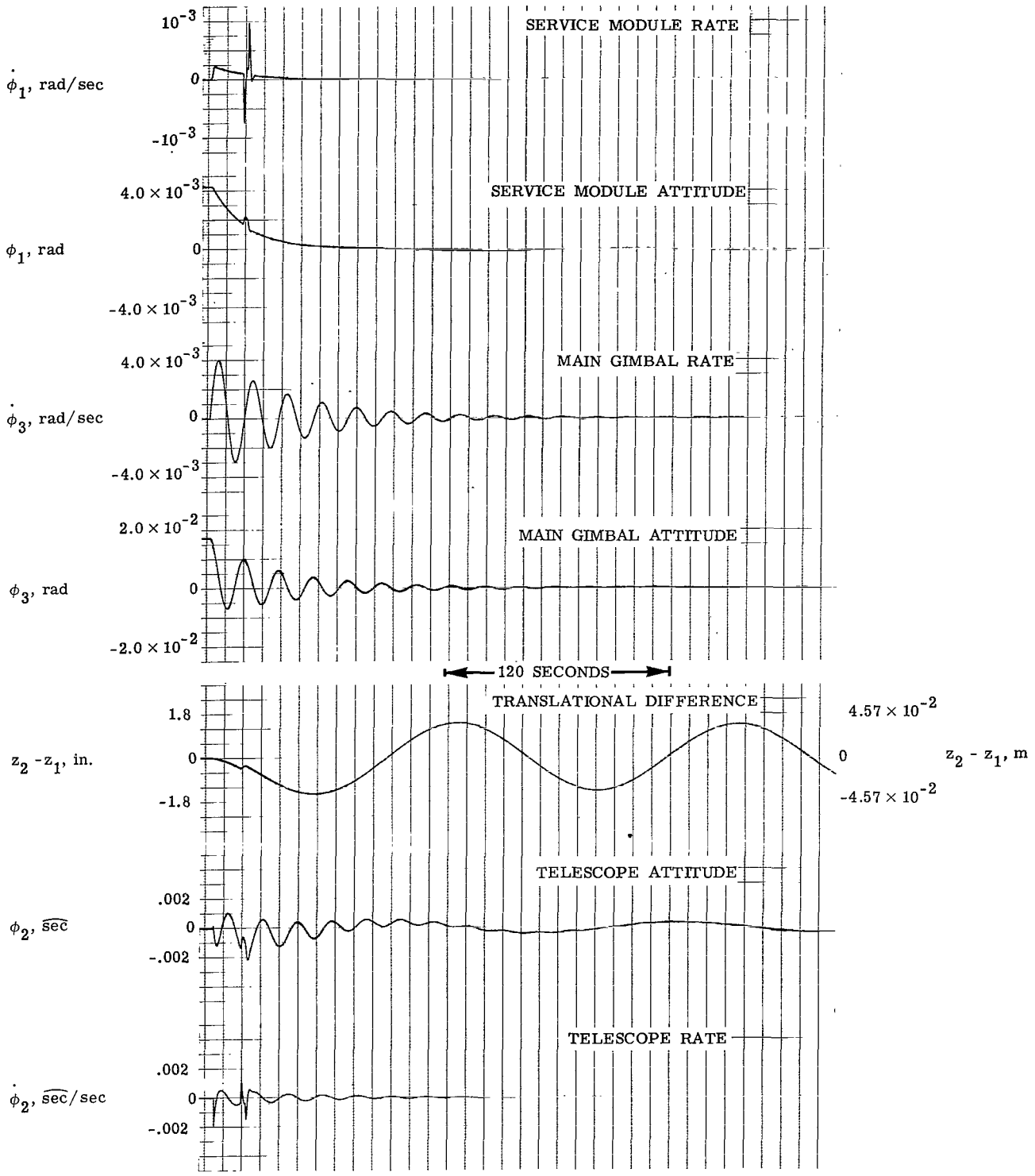

Figure 11.- Response of vehicle to crew-motion disturbance and initial conditions of 1^0 on main-gimbal attitude and 0.25^0 on service-module attitude. CMG gimbal set at 0^0.

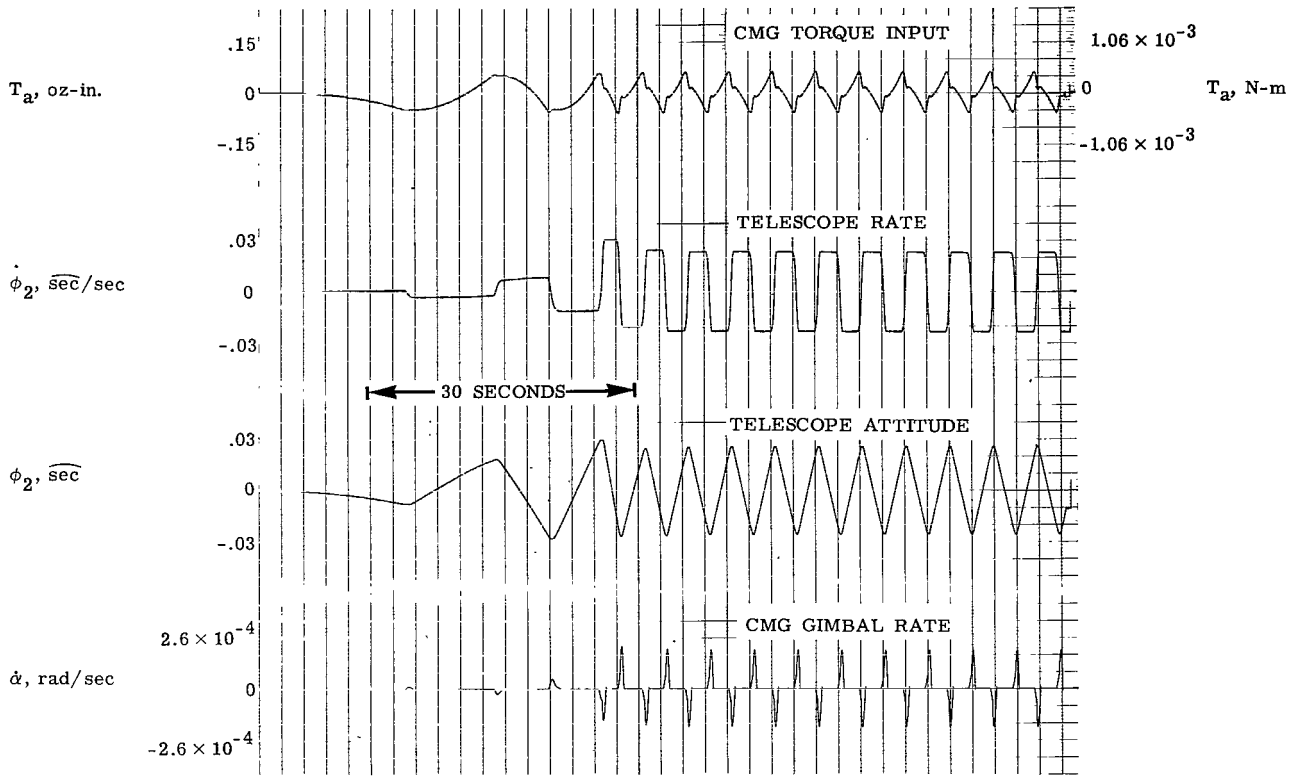

Figure 12.- Limit cycle in telescope control system for disturbance torque input of zero. CMG gimbal set at 0^0.

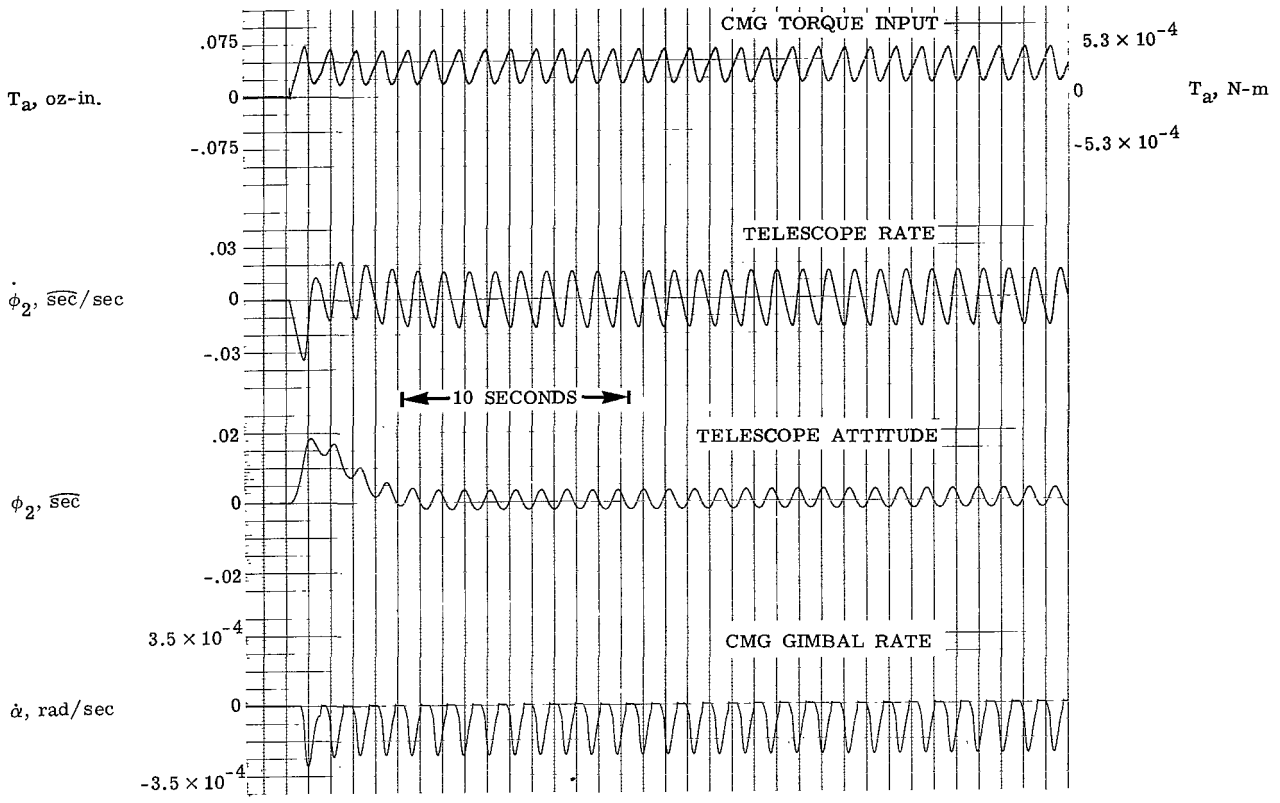

Figure 13.- Limit cycle in telescope control system for step input of 0.0455 lb-ft (6.2 × 10^{-2} N-m). CMG gimbal set at 0°.

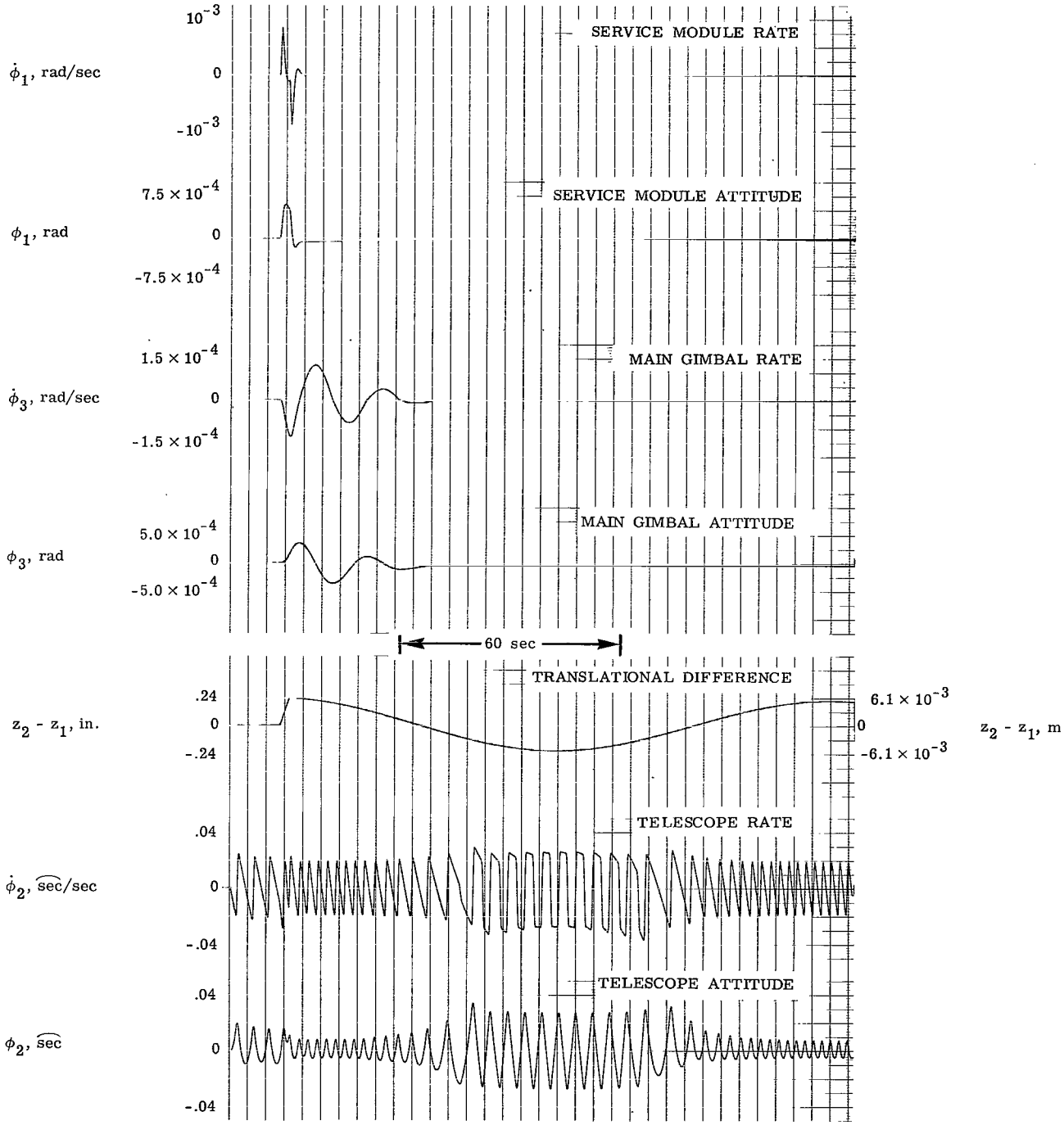

Figure 14.- Response of vehicle to crew-motion disturbance. Step input on telescope, 0.01 lb-ft (1.36×10^{-2} N-m); input on service module, 0.1 lb-ft (1.36×10^{-1} N-m). Main-gimbal and CMG nonlinearities included. CMG gimbal set at 45°.

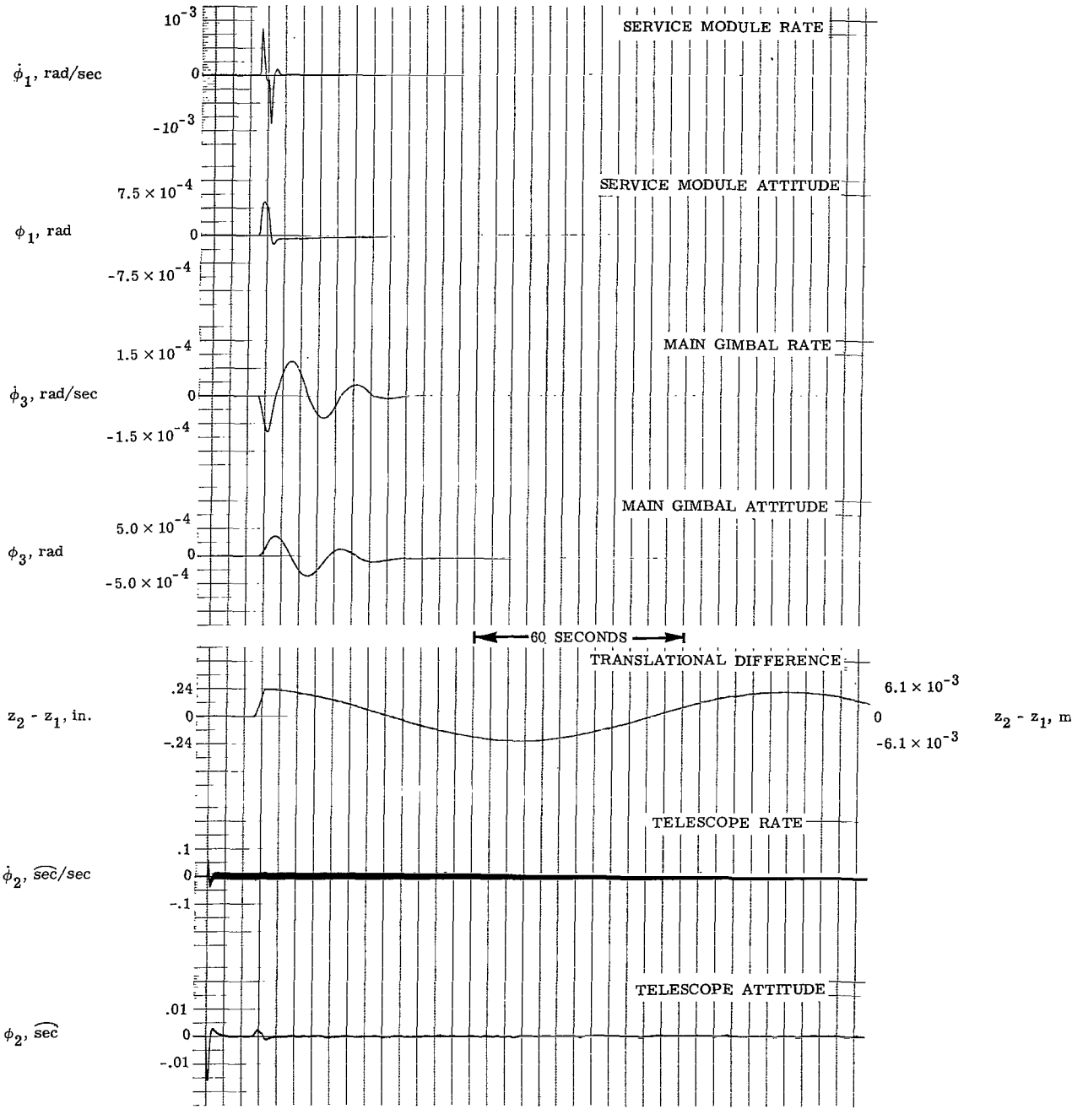

Figure 15.- Dither signal of 0.75 oz-in. (5.3×10^{-3} N-m) at a frequency of 38 rad/sec added to conditions of figure 14.

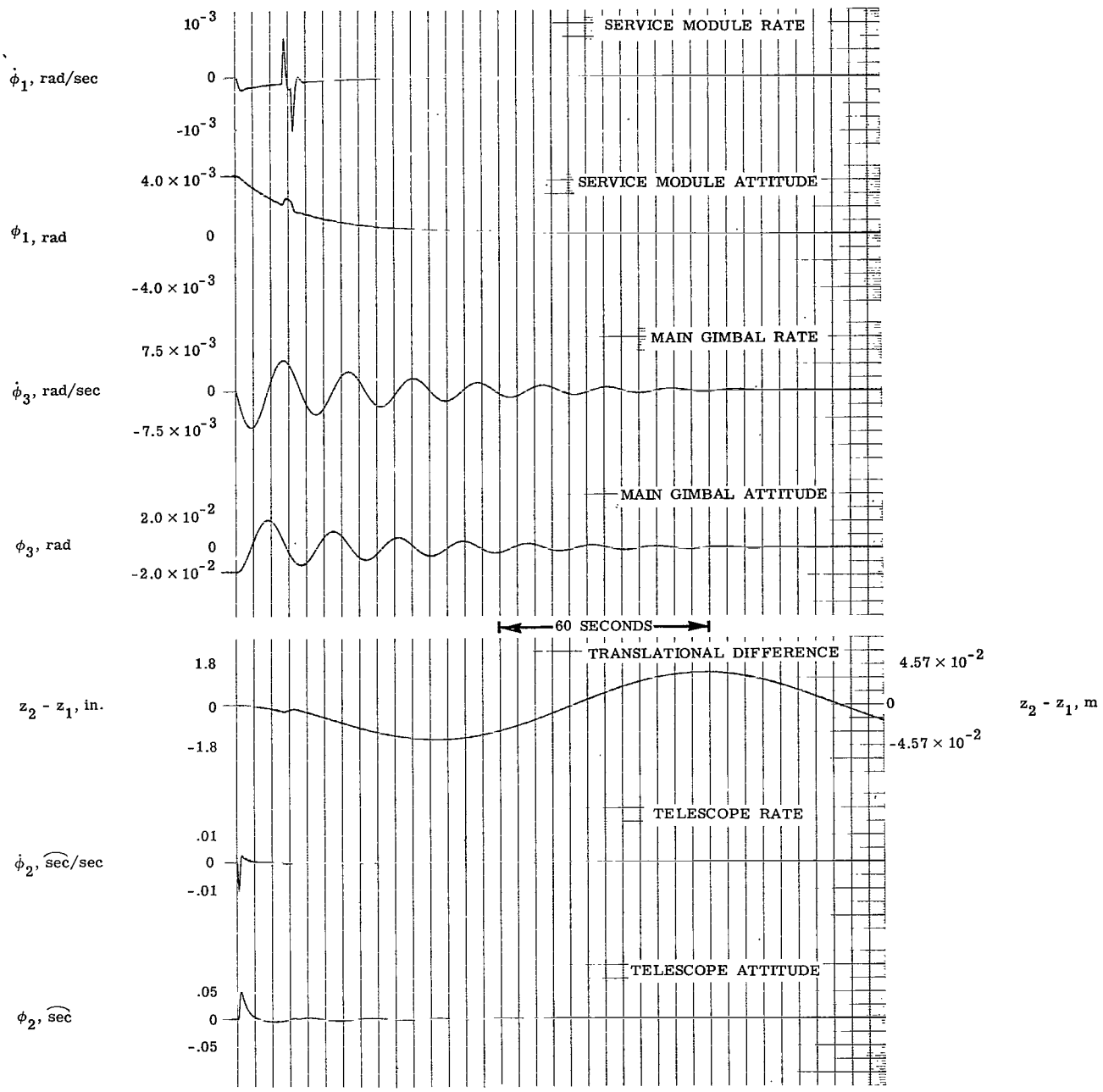

Figure 16.- Response of vehicle to crew-motion disturbance. Maximum environmental torques; initial conditions, 0.25^0 on service module and 1.0^0 on main gimbal. CMG and main-gimbal nonlinearities included. CMG gimbal set at 45^0.

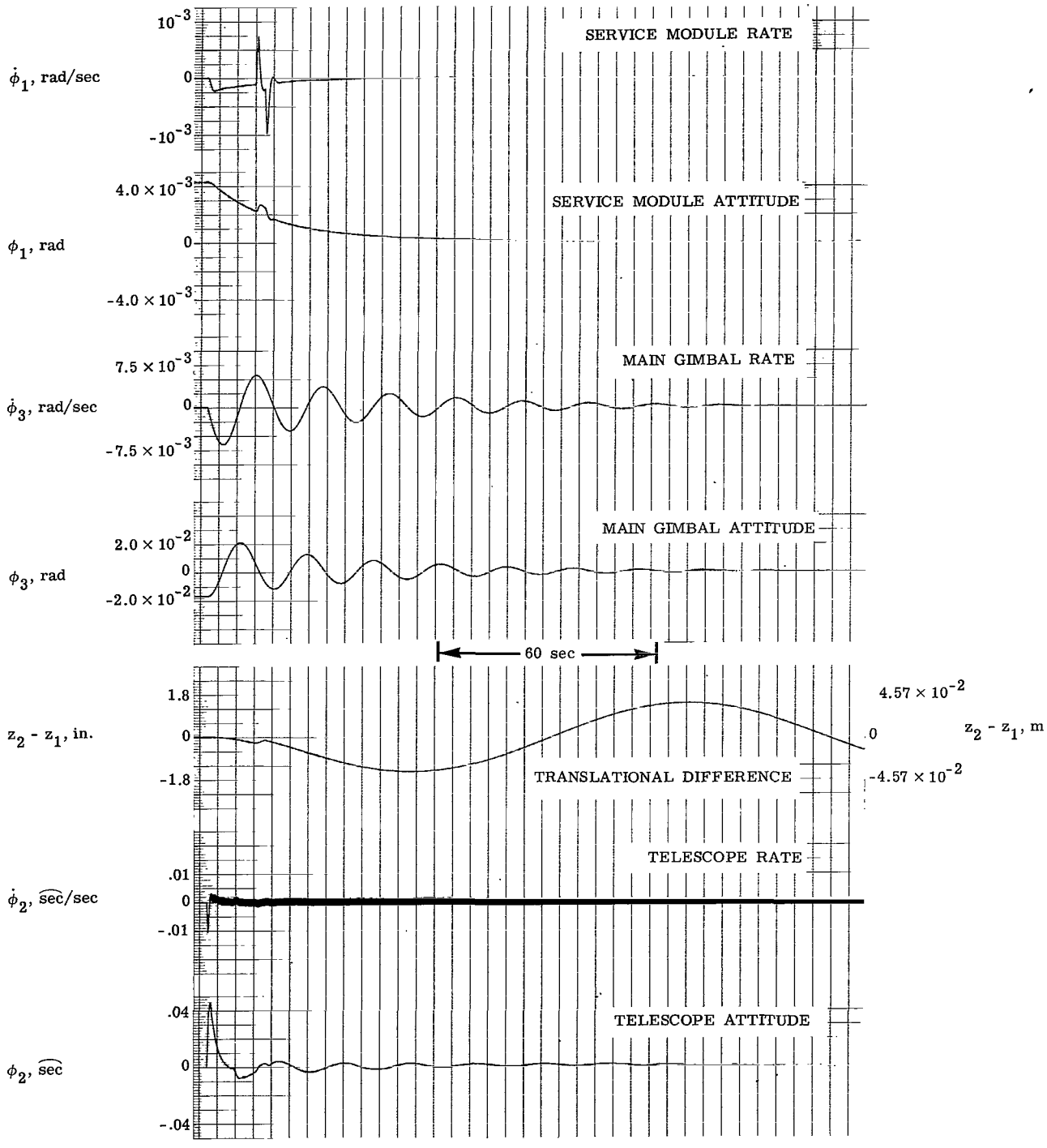

Figure 17.- Dither signal added to conditions of figure 16.

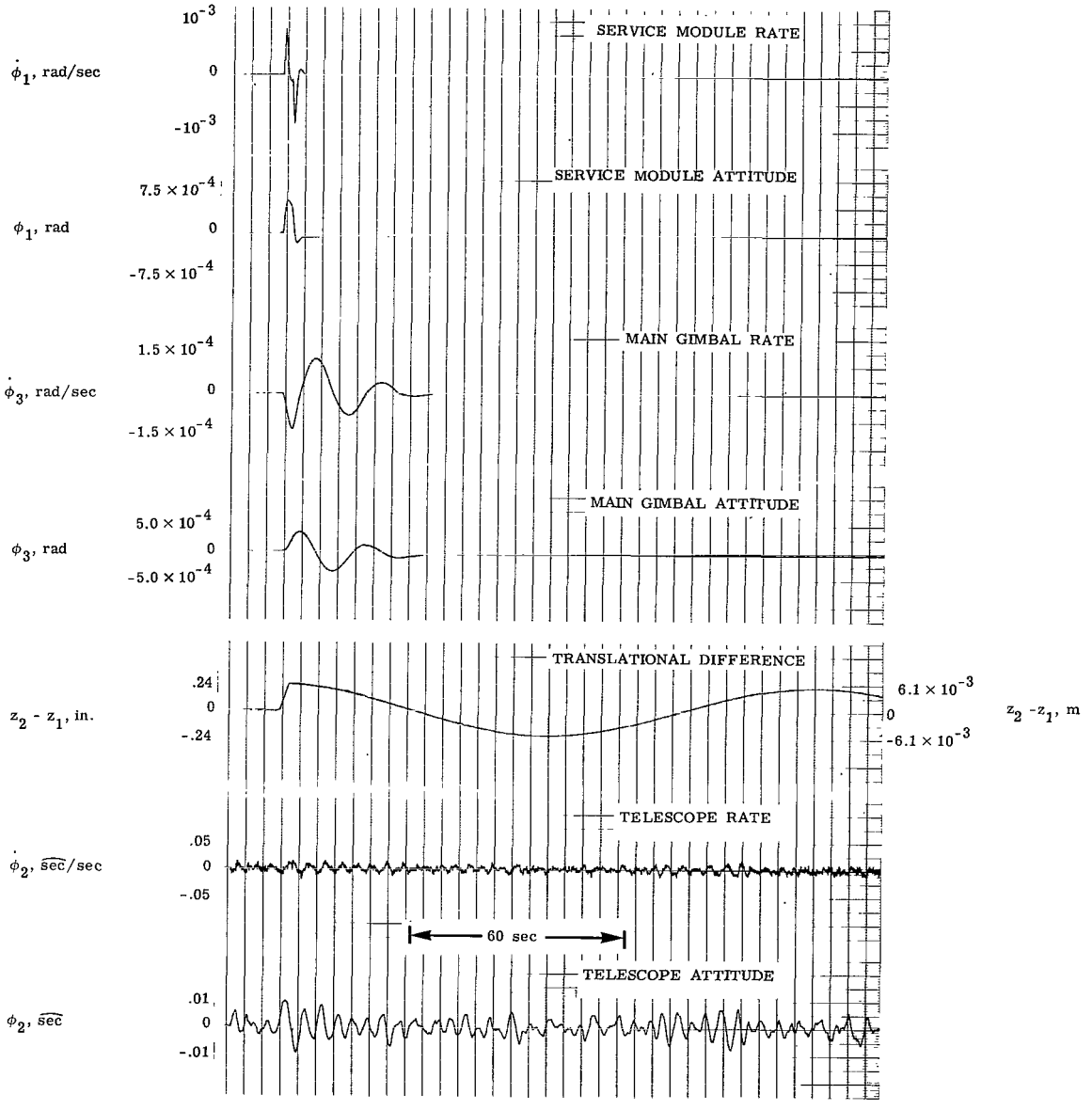

Figure 18.- Noise added to conditions of figure 14.

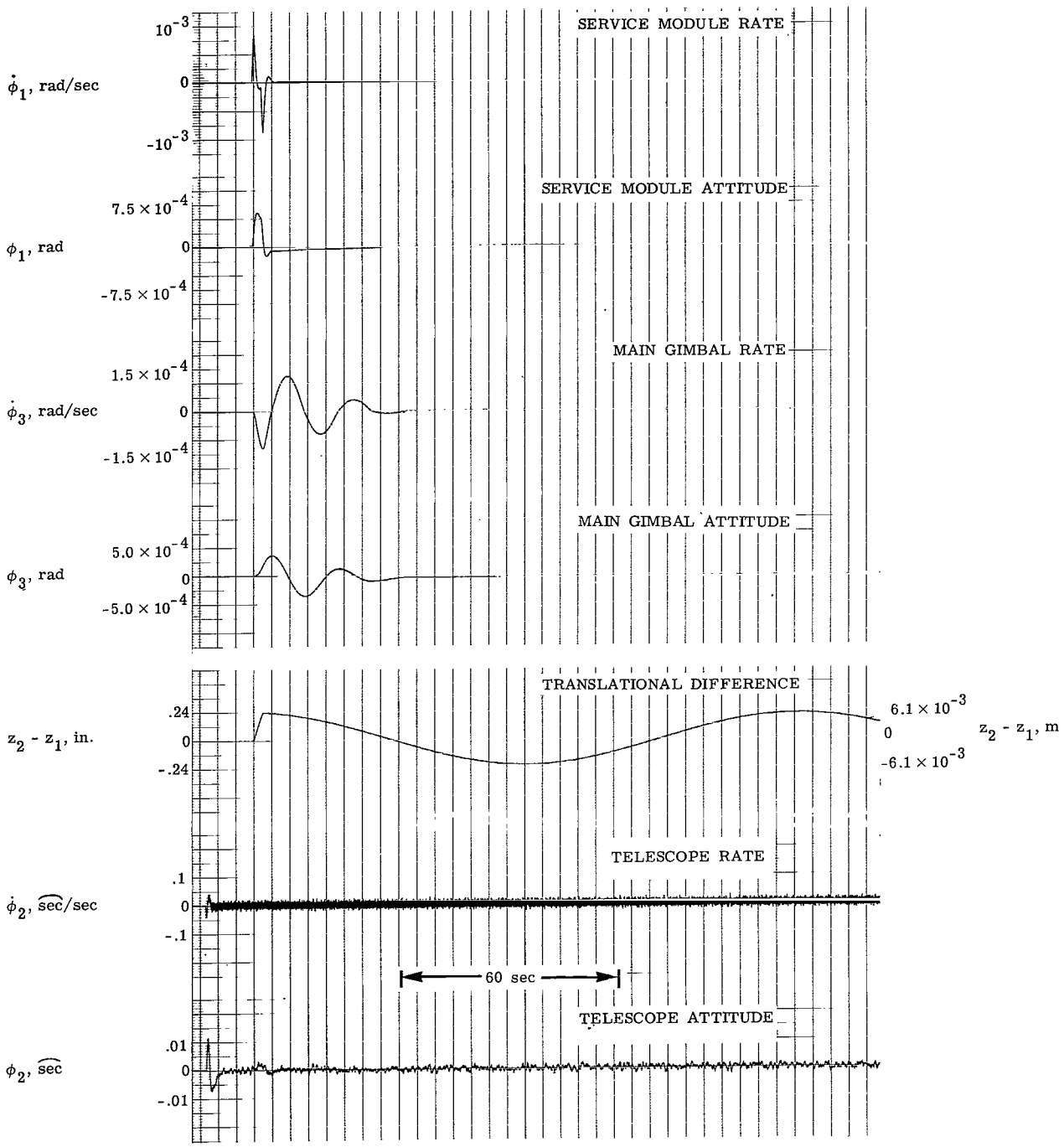

Figure 19.- Noise and dither added to conditions of figure 14.

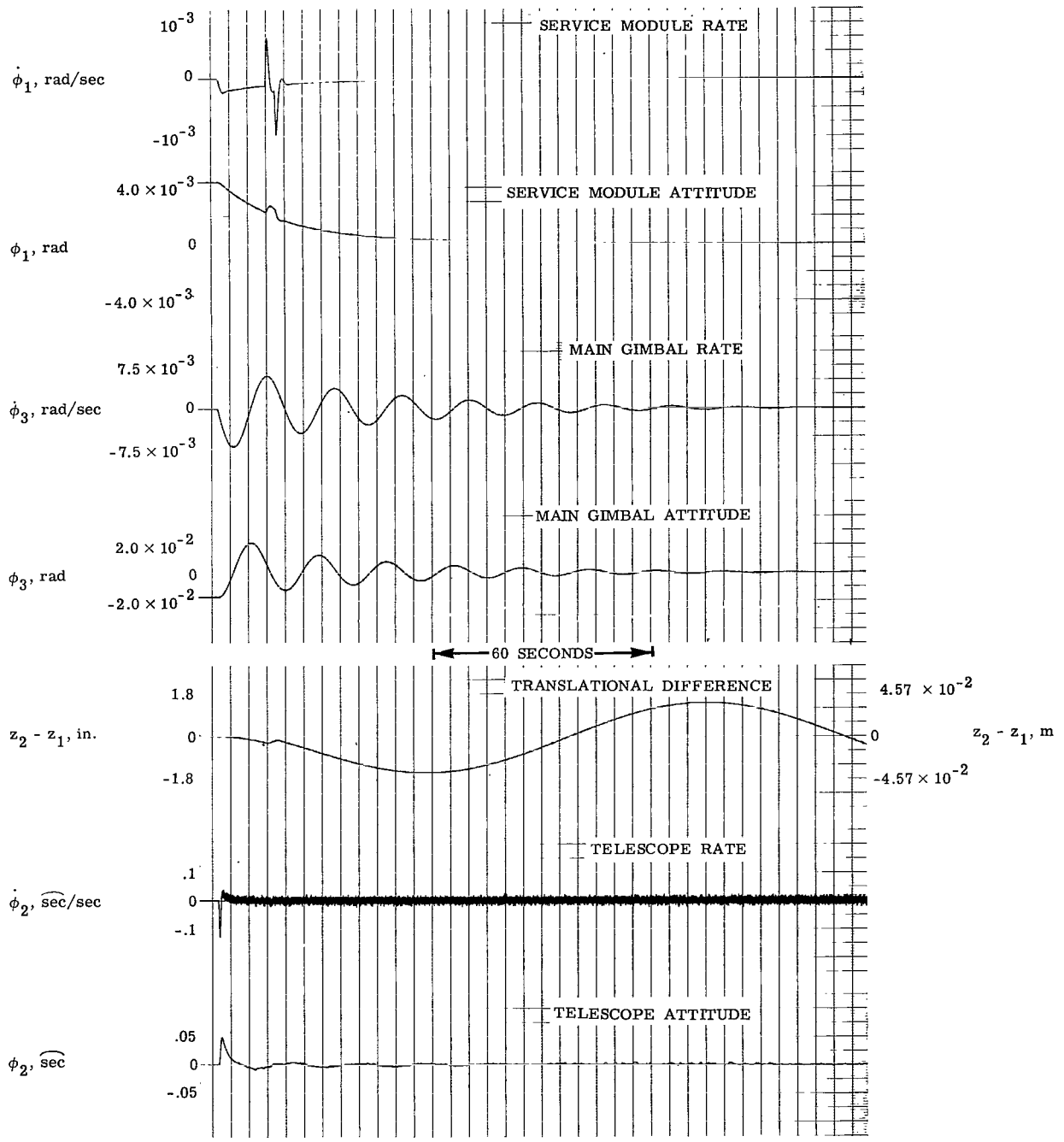

Figure 20.- Noise and dither added to conditions of figure 16.

NATIONAL AERONAUTICS AND SPACE ADMINISTRATION
WASHINGTON, D. C. 20546

OFFICIAL BUSINESS

FIRST CLASS MAIL

POSTAGE AND FEES PAID
NATIONAL AERONAUTICS AND
SPACE ADMINISTRATION

"The aeronautical and space activities of the United States shall be conducted so as to contribute . . . to the expansion of human knowledge of phenomena in the atmosphere and space. The Administration shall provide for the widest practicable and appropriate dissemination of information concerning its activities and the results thereof."

—NATIONAL AERONAUTICS AND SPACE ACT OF 1958

NASA SCIENTIFIC AND TECHNICAL PUBLICATIONS

TECHNICAL REPORTS: Scientific and technical information considered important, complete, and a lasting contribution to existing knowledge.

TECHNICAL NOTES: Information less broad in scope but nevertheless of importance as a contribution to existing knowledge.

TECHNICAL MEMORANDUMS: Information receiving limited distribution because of preliminary data, security classification, or other reasons.

CONTRACTOR REPORTS: Scientific and technical information generated under a NASA contract or grant and considered an important contribution to existing knowledge.

TECHNICAL TRANSLATIONS: Information published in a foreign language considered to merit NASA distribution in English.

SPECIAL PUBLICATIONS: Information derived from or of value to NASA activities. Publications include conference proceedings, monographs, data compilations, handbooks, sourcebooks, and special bibliographies.

TECHNOLOGY UTILIZATION PUBLICATIONS: Information on technology used by NASA that may be of particular interest in commercial and other non-aerospace applications. Publications include Tech Briefs, Technology Utilization Reports and Notes, and Technology Surveys.

Details on the availability of these publications may be obtained from:

SCIENTIFIC AND TECHNICAL INFORMATION DIVISION

NATIONAL AERONAUTICS AND SPACE ADMINISTRATION

Washington, D.C. 20546